Inhibition governs stimulus preference encoding in mPFC pyramidal neurons during a social choice

Renad Jabarin[1], Shai Netser[1] and Shlomo Wagner[1,*]

*Lead contact author: shlomow@research.haifa.ac.il

[1]Sagol Department of Neurobiology, Faculty of Natural Sciences, University of Haifa, Haifa, Israel

Summary

Social decision-making requires the brain to continuously evaluate competing options and select appropriate actions. The medial prefrontal cortex (mPFC) has been implicated in social cognition and value-based decision-making, yet the neural mechanisms by which it encodes the relative value of competing social choices remain poorly understood. Here, we employed fiber photometry, optogenetics, and projection-specific recordings in mice performing four distinct binary social discrimination tasks to reveal how mPFC pyramidal neurons encode social choice. We found that mPFC pyramidal neurons exhibit profound inhibition during bouts toward the preferred stimulus. This inhibitory response was specific to transitional bouts, when animals switched between stimuli, and was absent during non-transitional bouts, which occurred during continued engagement with the same stimulus. Notably, this differential activity encoded relative rather than absolute stimulus value, such that the same stimulus evoked opposite neural responses depending on its contextual preference. Accordingly, manipulating the subject's preference between food and social stimuli via food deprivation inverted its inhibition-excitation pattern. Furthermore, negative calcium transients in the mPFC predicted subsequent investigation of the preferred stimulus, suggesting a functional role in guiding behavioral choice. Optogenetic activation of mPFC pyramidal neurons during stimulus investigation produced immediate aversion yet paradoxically biased the stimulated animal to persistently re-engage with the stimulus-associated option through repetitive non-transitional bouts. Finally, projection-specific recordings revealed that mPFC neurons targeting the nucleus accumbens and basolateral amygdala were differentially recruited across tasks, reflecting functional specialization of output pathways. Together, these findings identify inhibition of mPFC pyramidal neurons as a key neural signature for encoding relative stimulus preference, thereby establishing a neural principle by which the mPFC dynamically guides social choice.

Key words: Medial prefrontal cortex (mPFC), social decision-making, value encoding, pyramidal neurons, fiber photometry, optogenetic manipulations, neural inhibition.

Introduction

Social interactions are fundamental to the survival and well-being of many species, including humans. These interactions are composed of a continuous stream of decisions that require an individual to evaluate available social partners, interpret their intentions, and select appropriate actions [1, 2]. Thus, social decision-making is a complex cognitive function that relies on the brain's ability to assign value to different social stimuli and to flexibly adapt behavior in response to a constantly changing social landscape [3]. A breakdown in this critical capacity can lead to profound social deficits, as seen in a variety of neuropsychiatric and neurodevelopmental disorders, most notably autism spectrum disorder (ASD) [4, 5].

The medial prefrontal cortex (mPFC) has emerged as a critical hub in the neural circuitry governing social cognition and value-based decision-making [6, 7]. Extensive research in both humans and animal models has identified the mPFC as a critical regulator of a wide range of social functions, including the recognition of conspecifics, the interpretation of social cues, and the regulation of the approach–avoidance balance [8-10] and the integration of emotional and contextual cues [11]. It has been proposed that the mPFC's function is to learn and represent associations between context and adaptive behavioral responses, a principle that may extend from simple reward-based tasks to the complex, dynamic world of social interaction [12, 13]. Understanding this process is crucial for deciphering how the brain dynamically navigates the complexities of the social world—a process that remains poorly understood

While it is well established that the mPFC encodes context-dependent value in non-social operant tasks involving explicit rewards or costs [14], it remains unclear whether similar principles govern the more fluid and spontaneous nature of social interactions. In natural settings, the 'value' of a social partner is not fixed but rather dynamically shaped by the presence of other individuals, the subject's internal state, and the broader social environment [15, 16]. This concept of relative valuation is a hallmark of flexible and adaptive decision-making. However, a central and unanswered question in social neuroscience is how the mPFC dynamically encodes the relative appeal of social choices, particularly during innate behavior and unconditioned social contexts.

At the circuit level, decision-making is often conceptualized as a competition between neuronal populations that is resolved through a balance of excitatory and inhibitory signaling, ultimately biasing activity in favor of one option over another [17-21]. The

mPFC is thought to implement this process through a 'differential coding' scheme, where distinct patterns of neural activity represent different types of social information [10, 22]. Despite these advances, a significant gap remains in our understanding of how the mPFC translates the relative value of social options into a concrete behavioral choice. While we know that the mPFC is involved, we do not yet have a clear understanding of the neural code that represents the decision itself, nor do we comprehend how this code is utilized to guide the initiation, maintenance, and switching of social investigation [23, 24]. Specifically, it is still unknown how the mPFC dynamically encodes the relative value of competing social and non-social options and how this evolving representation translates into behavioral choice [25, 26].

Here, we use a battery of four distinct social discrimination tasks in mice, each requiring a choice between two stimuli of varying motivational value, to show that the mPFC encodes the relative value of social choices through selective inhibition: pyramidal neurons are profoundly inhibited during transitional bouts toward the preferred stimulus, distinguishing it from both the non-preferred stimulus and baseline chamber investigation. This differential activity was observed specifically during transitional bouts between stimuli, suggesting a role in the decision to engage with a new option. Furthermore, we found that negative calcium transients in the mPFC were predictive of subsequent investigation of the preferred stimulus. Furthermore, distinct mPFC projections to the NAc and BLA were differentially engaged during social decisions, indicating that valuation and emotional discrimination are mediated through segregated downstream circuits. Finally, optogenetic activation of mPFC pyramidal neurons during stimulus investigation, despite eliciting an immediate avoidance, was sufficient to bias choice by increasing the preference for the stimulated option via repetitive bouts of investigation. Together, these findings identify a neural principle underlying social choice encoding in the mPFC and demonstrate how cortical circuits transform social information into adaptive decisions.

Results

I. Behavioral characterization of social choice across multiple binary discrimination tasks

To establish a behavioral framework for interpreting neural activity in the mPFC, we first assessed how subject mice behave when faced with a binary choice between distinct stimuli with varying motivational value. To that end, adult males were tested in four different discrimination tasks that required them to choose between two distinct stimuli.

In the Social Preference (SP) task, subject mice were exposed to a novel age- and sex-matched conspecific (social stimulus) on one side of the arena and an inanimate object on the other side (Fig. 1A), and exhibited a higher preference to investigate the social stimulus over the object, as reflected by their investigation time (Fig. 1B-C) and mean investigation bout duration (Fig. 1D) for each of the stimuli. In the Sex Preference (SxP) task, subjects preferred to investigate a female over a male conspecific (Fig. 1F-I). In the Emotional State Preference for stress (ESPs) task, subjects preferred a stressed over a naïve conspecific (Fig. 1K-N). Lastly, in the Social vs. Food (SvF) task, subjects displayed a significant preference for a conspecific over food (Fig. 1P-S). While the four tasks represent distinct social contexts, they all exhibit a similar level of stimulus preference, as reflected by the relative discrimination index (RDI; Fig. S1A). Notably, all four tasks shared one type of stimulus – a novel naïve male, which was the preferred stimulus in the SP and SvF tasks, but was the non-preferred stimulus in the SxP and ESPs tasks.

The four tasks also exhibited a similar level of social propensity, as reflected in the total investigation time (Fig. S1B) and showed a similar distance traveled during each task (Fig. S1C). Thus, they appear to induce a comparable level of social motivation and arousal in the subject animals, and differ primarily in the type of choice, dictated by the identity of the presented stimuli.

We then differentiate between two types of investigation bouts presumably differing in the type of decision preceding them: transitional vs. non-transitional. Transitional bouts occur when the subject animal investigates one stimulus following a previous bout with the other stimulus. As we previously described [27], transitional bouts were more abundant at the early stage of each of the four tasks, with no apparent correlation with the investigation time (Fig. 1B,G,L,Q, grey line). They reflect the animal's decision to stop investigating one stimulus and start investigating the other stimulus, thus performing a behavioral shift. In contrast, non-transitional bouts occur when the subject

animal investigates one stimulus following a previous bout with the same stimulus, hence reflecting the sustained tendency of the animal to pursue the same stimulus.

We found that in all four tasks, mice exhibited a greater number of non-transitional bouts compared to transitional bouts (Fig. S1D). Moreover, we found a significantly higher number of non-transitional bouts for the preferred stimulus over the non-preferred stimulus in all tasks, except for the SvF, where only a trend was observed (Fig. 1E,J,O,T). These findings suggest that mice exhibit a consistent tendency to persist in investigating the preferred stimulus once it has been selected, and that social decision-making involves both sustained engagement and selective switching between options.

II. Activity of mPFC pyramidal neurons discriminates between transitional and non-transitional bouts

To examine the activity of mPFC CaMKIIα-expressing pyramidal neurons during the four social discrimination tasks, we employed fiber photometry, as previously described [28]. For that, we injected the mPFC with AAV viral vectors to express the genetically encoded calcium indicator GCaMP6f under the control of the CaMKIIα promoter (Fig. 2A). We then recorded calcium signals from subject mice during the experiments shown in Fig. 1, with each session comprising a 10-minute recording of calcium signals: five minutes before the introduction of stimuli into stimulus chambers (pre-encounter phase) and five minutes after it (encounter phase, see timeline in Fig. 2B). Example traces of normalized calcium signal aligned with the onset of non-transitional and transitional bouts performed during that session, as well as mean traces for each of the four tasks are shown in Fig. S2A-H.

We used z-score Analysis to normalize and average all the instantaneous signals recorded during the two types of behavioral events—namely, transitional and non-transitional bouts—separately. We then analyzed the averaged z-scored calcium response for each behavioral event across all sessions of the same task, as previously described by us [28].

We first determined the responses of mPFC pyramidal neurons during transitional and non-transitional bouts of investigation conducted toward the two empty stimulus chambers during the pre-encounter phase of each session. No behavioral preference was found for one empty chamber over the other in any of the four tasks (Fig. S3A-D). Still, we found that both non-transitional bouts (in SP, SxP, and ESPs tasks; Fig. S3E-F) and transitional bouts (in all four tasks; Fig. S3G-H) elicited an immediate increase in the recorded signal (mainly during -1 to 2s relative to the beginning of the bout), with this

excitatory response being more robust in transitional compared to non-transitional bouts (Independent t-test- -1to2s: $t(45)=-5.35$, $p<0.001$; 3-6s: $t(45)=-1.572$, $p=0.117$).

We then analyzed the responses of mPFC pyramidal neurons during the encounter stage of the various sessions, when subject mice investigated stimulus-containing chambers. Importantly, we compared these responses with the signals recorded during transitional and non-transitional bouts toward the empty chambers during the pre-encounter stage. We found that transitional bouts elicited differential neural responses between the two stimuli, with the preferred stimulus eliciting a significant inhibition while the non-preferred one eliciting excitation. Nevertheless, there was no difference between the excitatory response toward the non-preferred stimulus and the response toward the empty cages during the pre-encounter stage, while the inhibitory response toward the preferred stimulus showed a significant difference from the empty chamber response in all tasks (Fig. 2C-N). In contrast, we found that across all four tasks, non-transitional bouts during the encounter stage did not show any difference in the response between the stimuli (Fig. O-R, Fig. S4A-H). These results, which are further apparent when all four tasks are averaged (Fig. 2S-T), suggest that a differential response between the two stimuli occur in mPFC pyramidal neurons only during transitional investigation bouts, but not during non-transitional bouts. They also suggest that it is the preferred stimulus that elicit an inhibitory response during transitional bouts, while the excitation observed during non-preferred stimulus investigation is a generic response during chamber investigation.

III. Context-Dependent Encoding of Relative Stimulus Value in the mPFC

Our results so far show that mPFC CaMKII neurons are differentially responsive to investigation bouts following a behavioral shift, where the animal leaves one stimulus in order to investigate the other stimulus, and are less responsive to investigation bouts that involve repeating the same action consecutively. Yet, this differential response may be sensitive to the absolute appeal of the stimulus, determined by its identity, or to its relative appeal, determined by the other option (stimulus) presented in the same context, rather than by the specific identity of the stimulus itself.

As motioned above, all four tasks used by us shared a common stimulus - a naïve male conspecific. However, the preference for this stimulus differed between the tasks: it was the preferred stimulus in the SP and SvF tasks, while in SxP and ESPs tasks it was the non-preferred stimulus, as shown by the RDI values (Fig. S3A). Despite the identical

nature of this common stimulus across the four tasks, mPFC pyramidal neurons activity during transitional bouts toward this stimulus depended on whether the stimulus was the preferred or the non-preferred in that given task (Fig. 3B-C). Specifically, neural activity during transitional bouts toward the common stimulus was mostly inhibitory in sessions where the common stimulus was the preferred stimulus (RDI > 0), while in sessions where it was the non-preferred stimulus (RDI < 0) the neural activity was excitatory (Fig. 3D). This difference was specific for transitional bouts and was not detected during non-transitional bouts (Fig. 3E-F).

To test directly whether the observed inhibition of mPFC pyramidal neurons in transition bouts is indeed related to the relative appeal of the stimulus rather than its identity, we examined how the neural activity of mPFC pyramidal neurons changes when stimuli identity is held constant but their relative appeal is altered. To that end, we recorded animals performing the SvF task following 24 hours of food deprivation (Fig. 3G). As expected, animals exhibited a strong preference for the food over the social stimulus, as reflected by the time dedicated to investigate each stimulus and the number of non-transitional bouts (Fig. 3H-I). Accordingly, RDI values were significantly different between satiety and food deprivation (Fig. 3J). This change in preference was accompanied by a "flip" in the neural activity pattern observed in the SvF task during food deprivation, as compared to satiety (Fig. 3K-P). Specifically, transitional bouts toward the food elicited inhibitory responses, as compared to excitatory responses to the social (common) stimulus (Fig. 3P). Moreover, the responses during transitional bouts to the same stimulus, whether food or social, were opposite between satiety, when the social stimulus was preferred, and food deprivation, where food was the preferred stimulus (Fig. 3Q-R). These results further demonstrate that the mPFC neurons differential response during transitional investigation bouts depends on the relative appeal of the stimulus, with an inhibitory response elicited specifically by the preferred stimulus.

The relationship between inhibited activity of mPFC pyramidal neuron activity and social preference was further assessed by calculating the probability of social investigation following significant negative or positive changes in calcium activity (Fig. S5A-L). This Analysis revealed that negative calcium transients are predictive of the subjects' behavior in all four tasks, given that they were followed by a statistically significant increased probability of investigation behavior toward the preferred stimulus, but not toward the non-preferred stimulus (Fig. 4A-P). Moreover, this increase in

probability during the encounter was significantly higher than that recorded during the pre-encounter stage, suggesting that the negative transients are associated with the investigation of the preferred stimulus. In contrast, no such significant change from baseline or the pre-encounter stage was recorded for positive transients (Fig. 4Q-R, Fig. S6A-H).

Together, these findings suggest that decreased activity of mPFC pyramidal neurons serves a functional role in regulating investigation behavior toward the preferred stimulus and can be predictive of the animal's stimulus investigation behavior.

IV. Optogenetic Stimulation of mPFC Pyramidal Neurons During Stimulus Investigation Modulates Social Choice in a Context-Dependent Manner

To further examine whether pyramidal neurons of the mPFC play a critical role in mediating social choice, we used optogenetic stimulation to activate these neurons during stimulus investigation. For that, we used AAV viral vectors to express the excitatory opsin Channelrhodopsin-2 (ChR2) under the control of the CaMKIIα promoter in the mPFC, followed by optic fiber implantation for blue light delivery (Fig. 5A). Photo-stimulation (7–10 ms pulses at 10 Hz) was delivered specifically during investigation bouts toward a given stimulus (from onset to end of bout, Fig. 5B). Each task was repeated three times under three distinct stimulation protocols: no stimulation, stimulation during bouts with one stimulus, and stimulation during bouts with the other stimulus. Notably, there were no differences in the total investigation time between the four tasks in the "no stimulation" condition, indicating a similar level of social motivation without stimulation (Fig. S7A).

We found that optic stimulation delivered during investigation bouts with the preferred stimulus strengthened the preference toward it in SP, ESPs, and SvF, while merely preserving it in the SxP task, as reflected by the investigation time (Fig. 5C,H,M,R) and RDI (Fig. S7B-E). Conversely, stimulating the mPFC during bouts toward the non-preferred stimulus changes the subject's preference, abolishing it in specifically in the SP task and reversing it to create a preference toward the typically non-preferred stimulus in the SxP, ESPs, and SvF tasks. Thus, stimulating mPFC pyramidal neurons during stimulus investigation seem to enhance the investigation of that stimulus.

We then examined how optic stimulation of mPFC pyramidal neurons affects the structure of stimulus investigation. We first analyzed the time course of all investigation bouts toward a given stimulus and, to our surprise, found that in almost all cases

(besides SvF) the optic stimulation shortens the mean investigation bout rather than lengthening it (Fig. 5D-E,I-J,N-O,S-T). We then examined the number of transitional and non-transitional bouts toward each stimulus in all three stimulation conditions. In most cases we found a significantly greater number of non-transitional bouts toward the stimulus paired with optic stimulation, while the transitional bouts were affected less consistently (Fig. 5F,K,P,U; Fig. S7F-M). Accordingly, the ratio between non-transitional to transition bouts was always significantly higher for the stimulation-paired stimulus compared to the other stimulus (Fig. 5G,L,Q,V). Moreover, the ratio of non-translational bouts to all bouts pulled across all tasks wag significantly higher for the stimulation-paired stimulus compared to the other stimulus or non-stimulation condition (Fig. 5W), suggesting that optic stimulation elicit a high level of repetitive investigation bouts toward the stimulation-paired stimulus.

We next tested whether the effect of mPFC pyramidal neuron activation was specific to social contexts, by delivering optic stimulation during investigation bouts with an empty chamber. We found that subject animals exhibited a preference for the empty chamber coupled with optic stimulation (Fig. S8A-I). Thus, it seems as if stimulation of the mPFC pyramidal neurons exerts a mixed effect on the subject's investigation behavior, regardless of the stimulus nature: on one hand it shortens the investigation bouts, which may reflect avoidance toward the stimulus, but on the other hand it increases the number of non-transitional investigation bouts and made them more repetitive, which may reflect persistent interest in the stimulus. In order to farther examine this effect, we looked at the video recordings of the experiments and found that following the stimulation that was activated at the beginning of an investigation bout, subject animals rapidly stopped investigating the stimulus, but immediately after the termination of stimulation they started a new investigation of the same stimulus, a sequence that repeated itself several times before the animal made a transition and turned to investigate the other stimulus (Supp. Movie 1-2).

Taken together, the results of the optogenetic stimulation demonstrate that activation of mPFC pyramidal neurons exerts an immediate aversive effect on social investigation, prompting the subject to abruptly terminate its ongoing interaction with the stimulus. However, this manipulation does not alter the motivational drive of the subject to investigate that stimulus. Consequently, once the optic stimulation is terminated, subject animals are more likely to resume investigating the same stimulus (i.e., perform a non-transitional bout) to satisfy their initial motivation for investigating the stimulus, leading to

a counter-intuitive increase in the investigation time for that stimulus (see cartoon in Fig. 5X).

V. Functional Dissociation of mPFC Projections' Role in Mediating Social Choice

So far, we examined the activity of the whole population of mPFC pyramidal neurons. However, sub-populations of these neurons project to several distinct brain regions [29], hence may have different principles organizing their activity during a binary choice between stimuli. Therefore, we examined the activity of two such sub-populations: those that project to the nucleus accumbens (NAc) and those that project to the basolateral amygdala (BLA), during the same four tasks used by us so far. To target mPFC neurons projecting to a given region we injected a retrogade CAV-Cre viral vector mixed with an AAV vector expressing mCherry (to label the injection site) into either the NAc or the BLA. We also injected into the mPFC an AAV vector leading to the expression of GCaMP7 under the human EF1α promoter in a Cre-dependent manner (Fig. 6A-B). Upon recovery, we used fiber photometry to record calcium signals while subject animals performed the four tasks, as described above.

In the SP, SxP, and ESPs tasks, subject animals of both groups (mPFC-to-NAc and mPFC-to-BLA) displayed a similar preference as reported earlier for the CaMKII-GCaMP-injected animals in SP, SxP, and ESPs tasks (Fig. 6C,E,G,I,K,M). In the SvF task, however, subject animals from both groups displayed no preference for either stimulus (Fig. 6O,Q).

We next examined the neural activity of mPFC-to-NAc and mPFC-to-BLA projecting neurons during non-transitional and transitional bouts in each task. In all four tasks, both populations of mPFC projecting neurons exhibited no differential responses during non-transitional bouts to either of the stimuli. Similar to the general population of pyramidal neurons, differences in neural responses—when present—were only found during transitional bouts. Yet, these differential responses were task-dependent.

In the SP task, both populations of projecting neurons exhibited a similar pattern of activity changes during transition bouts, with inhibitory responses to the social stimulus specifically in transitional bouts (Fig. 6D,F). In the SxP task, neither population showed any significant response during transitional bouts (Fig. 6H,J). In ESPs, only mPFC-to-BLA projecting neurons showed inhibitory response during transitional bouts with the

stressed stimulus (Fig. 6L,N). Conversely, In the SvF task only the mPFC-to-NAc projecting neurons population exhibited inhibitory responses during transitional bouts with the social stimulus compared to the food (Fig. 6P,R).

Taken together, the mPFC-to-NAc and the mPFC-to-BLA projecting neurons exhibit distinct pattern of responses during social choice in a task-dependent manner. Although their engagement varies across tasks, whenever these projections are recruited, their response profile follows the same consistent pattern observed in the broader CaMKII+ neuronal population: inhibition during transitional bouts toward the preferred stimulus.

Discussion

Social decision-making is a cornerstone of adaptive behavior, requiring the continuous evaluation of social cues and leading to selection of appropriate actions. Here, we provide compelling evidence that the mPFC plays a central role in this process by encoding the relative value of social choices through a context-dependent activity pattern. Our principal finding is that mPFC pyramidal neurons exhibit profound inhibition during transitional bouts toward a preferred stimulus, a response that is not only specific to the preferred option but also predictive of future choices. Such selective inhibition, coupled with a non-specific excitation during investigation of non-preferred stimuli, reveals a complex neural mechanism for social choice that is dynamically updated based on the relative appeal of available options.

Our results show that the mPFC does not encode the absolute identity of a social stimulus, but rather its relative value within a given context, as demonstrated by the "flipping" of the neural response to the same naïve male stimulus, which elicited inhibition when it was the preferred option (in the SP and SvF tasks) but excitation when it was non-preferred (in the SxP and ESPs tasks). These findings are consistent with our previous work on emotion recognition, where we observed inhibition of PrL pyramidal neurons during investigation of emotionally aroused individual, which is preferred over a naïve individual [28]. Context-dependent encoding was further confirmed by the SvF task, where the social stimulus elicited inhibition under satiety conditions (when it was the preferred option), but excitation following 24 hours of food deprivation (when food was the preferred option). **Such modulation of the neural response demonstrates** that the mPFC's encoding of social value is not fixed but rather modulated by the animal's internal motivational state, suggesting that inhibition of pyramidal neuronal activity may be a key mechanism by which the mPFC integrates internal state and external context to guide adaptive social choices. However, the exact neural circuit underlying the inhibitory and excitatory signals we observed remains to be fully elucidated. One possibility is that the inhibition of pyramidal neurons is mediated by local inhibitory interneurons, such as somatostatin (SOM) or parvalbumin (PV) interneurons. Recent work by Scheggia et al. (2020) [30] has demonstrated that SOM interneurons in the prefrontal cortex play a crucial role in discriminating between different affective states[22]. SOM interneurons may also be involved in the inhibitory signal we observed during interactions with preferred stimuli, perhaps by suppressing pyramidal neuronal

activity when the animal commits to a preferred option. Future studies using cell-type-specific manipulations will be necessary to test this hypothesis.

While previous work has established that the mPFC encodes value in non-social, operant tasks with explicit rewards [14, 31, 32], our findings demonstrate this principle in the context of free and spontaneous social interactions- a distinction that highlights a key advantage of our approach over conditioning paradigms. In operant tasks, animals are trained to associate specific stimuli with rewards or punishments, and the mPFC's role may be limited to executing learned associations. In contrast, our paradigms capture the mPFC's involvement in innate, spontaneous social discrimination, where animals must continuously evaluate and compare options without explicit training. These differences in behavioral context may explain why other operant task-based studies focusing on the mPFC during social approach have reported primarily excitatory responses [7, 16]. The inhibitory signal we observed appears specific to contexts where animals are making unconstrained choices between multiple options, as opposed to executing a learned response to obtain a reward, **suggesting** that the neural mechanisms underlying value encoding may differ fundamentally between spontaneous and conditioned social behaviors and underscoring the importance of studying social behavior in multiple settings.

Additionally, we found that the differential neural responses were primarily observed during transitional bouts, when the subject animal was switching between stimuli, and not during non-transitional bouts, which reflect sustained engagement. These findings suggest that the mPFC is particularly involved in the process of behavioral switching and reevaluation of choices, rather than in maintaining ongoing behavior. The inhibition observed during transitional bouts to the preferred stimulus may reflect a neural "reset" that facilitates the disengagement from the previous (non-preferred) option and the commitment to the new (preferred) one. The lack of differential activity during non-transitional bouts may indicate that once a choice is made and the animal is engaged in sustained investigation, the mPFC's role in value encoding becomes less critical, and other brain regions may take over the maintenance of the ongoing behavior. The distinction between transitional and non-transitional bouts is critical for understanding the dynamic nature of mPFC encoding. It demonstrates that the mPFC is not simply representing the value of a stimulus in a static manner, but is actively tracking the animal's behavioral state and updating its encoding based on the animal's previous decisions. Recent work by Gabriel et al. (2025) [33] supports this notion by showing that

prelimbic cortex population dynamics rapidly generate novel representations during action selection, with these representations emerging early in learning and predicting whether animals will take avoidance or exploratory actions. Such dynamic encoding is essential for adaptive behavior, as it enables the animal to remain flexible and responsive to environmental changes while maintaining stability once a choice has been made.

Our optogenetic experiments provide causal evidence for the role of mPFC activity in biasing social choice. Stimulating mPFC pyramidal neurons during the investigation of a stimulus enhanced the preference for that stimulus, regardless of its initial value. Paradoxically, the stimulation itself had an immediate aversive effect, causing the animal to cease social interaction and move away from the stimulus, which aligns with previous work showing that optogenetic stimulation of the mPFC can have negative or aversive effects on behavior, including enhanced fear associations and avoidance [13, 34-36]. However, upon termination of the optic stimulation, animals rapidly and repeatedly re-engaged with the same stimulus, as reflected in an increased number of non-transitional bouts. Such pattern of repetitive returns resulted in a net increase in total investigation time and a robust preference bias toward the stimulated option. Therefore, we propose that broad excitation in mPFC pyramidal neurons may serve as a "caution" signal, reflecting a state of heightened vigilance or alertness that, if passing a certain threshold, drives the animal to cease current behavior and explore alternatives. **The caution signal interpretation explains** why optogenetic stimulation of mPFC pyramidal neurons leads to immediate avoidance and shortened bout duration: artificial excitation may have mimicked a caution signal, prompting the animal to disengage from the social interaction prematurely. Supporting this interpretation, we observed an excitation effect during transitional bouts between empty chambers in the pre-encounter period, which was stronger than the effect found in non-transitional bouts. Transitional bouts, by definition, involve a shift from one stimulus to another, which may be a moment of heightened uncertainty or caution as the animal evaluates whether to commit to the new option. In contrast, non-transitional bouts reflect sustained engagement with a stimulus, a state in which the animal is naturally less cautious and more committed. By extension, the profound inhibition we observed during transitional bouts toward the preferred stimulus may reflect the suppression of this caution signal, effectively creating a "low-caution state" that permits the animal to commit to and engage in sustained social interaction with the preferred option. However, future experiments using optogenetic or

chemogenetic inhibition will be crucial for testing whether artificially inducing mPFC inhibition can create a low-caution state that promotes sustained investigation of any stimulus, regardless of its initial value.

Our recordings from mPFC neurons projecting to the nucleus accumbens (NAc) and basolateral amygdala (BLA) indicate that these projection-specific populations exhibit distinct functional specializations that depend on the behavioral choice context dictated by the type of stimuli. This finding aligns with a growing body of literature demonstrating functional specialization of mPFC output pathways. For instance, recent work has shown that mPFC-NAc projections specifically encode social winning behavior, while mPFC-BLA projections are more involved in processing negative emotional valence [37, 38]. The distinct responses we observed in mPFC-NAc and mPFC-BLA projecting neurons may reflect a division of labor, where one pathway signals the value of the chosen option to reward-related circuits, while the other signals the emotional or social context to valence-processing regions. Future studies using projection-specific manipulations will be necessary to determine whether the inhibitory signal we observed is specific to certain projection pathways and whether selectively manipulating these pathways can alter social choice.

Several limitations of our study should be acknowledged. First, while we targeted the mPFC, our viral injection and optic fiber implantation did not allow for a precise distinction between the prelimbic (PrL) and infralimbic (IL) subregions. Given the known functional heterogeneity of the mPFC, with the PrL and IL often playing distinct or even opposing roles in behavior [6, 12], our findings should be interpreted as reflecting the integrated activity of the mPFC as a functional unit. The PrL has been implicated in approach behavior and social cognition, while the IL is more often associated with avoidance and fear extinction [39]. It is possible that the inhibitory and excitatory signals we observed arise from different subregions, or that the relative contributions of PrL and IL vary depending on the specific discrimination task. Future studies using more targeted approaches, such as subregion-specific viral injections or localized optogenetic manipulations, will be necessary to dissect the specific contributions of the PrL and IL to social choice. Second, while our fiber photometry recordings revealed a strong correlation between mPFC inhibition and social choice, this technique does not provide the single-cell resolution needed to understand the underlying circuit dynamics in detail. Single-unit recordings or calcium imaging with cellular resolution will be necessary in

future studies to elucidate the precise interplay of excitatory and inhibitory neurons that gives rise to the observed population-level signals.

Our findings have several broader implications for our understanding of the neural basis of both typical and atypical social behavior. A hallmark feature of ASD is a disruption in the balance of excitation and inhibition (E/I balance) in cortical circuits, including the mPFC [21, 40]. This E/I imbalance has been proposed to underlie many of the core symptoms of ASD, including social deficits, repetitive behaviors, and sensory abnormalities. Our findings suggest that a disruption of the mPFC's value encoding mechanism—specifically, the inhibitory signal that marks commitment to a preferred social option—could contribute to the social choice deficits observed in ASD. If the inhibitory signal is weakened or absent, individuals with ASD may have difficulty committing to social interactions or may fail to appropriately prioritize social stimuli according to their value. Conversely, if excitatory activity is abnormally elevated, this could lead to a heightened "caution" signal that promotes avoidance of social interactions. Indeed, previous work has shown that restoring the balance of excitation and inhibition in the mPFC can rescue social behavior deficits in mouse models of ASD [40-42], suggesting that the integrity of mPFC circuits is crucial for normal social function. Future studies examining whether the context-dependent value encoding mechanism we observed is disrupted in mouse models of ASD will be important for understanding the neural basis of social deficits in this disorder and for developing targeted interventions.

In conclusion, our study provides novel insights into the neural mechanisms of social choice, demonstrating that the mPFC encodes the relative value of social options through a context-dependent inhibitory signal that is dynamically updated based on the subject's behavioral state and motivational context. These findings not only advance our understanding of the social brain but also provide a new framework for investigating the neural basis of social deficits in neuropsychiatric disorders.

Declarations

Acknowledgments

We thank Boris Shklyar, Head of the Bio-imaging Unit and Eng. Alex Bizer, the experimental systems engineer of the Faculty of Natural Sciences of the University of Haifa, for their technical help.

Author contributions

R.J.: Formal Analysis, Investigation, Methodology, Validation, Visualization, Writing - original draft, and Writing - review & editing; S.N.: Data curation, Project administration, Software, Validation, Visualization, Writing - original draft, and Writing - review & editing. S.W.: Conceptualization, Funding acquisition, Project administration, Resources, Supervision, Writing - original draft, and Writing - review & editing.

Competing interests

The authors declare that they have no competing interests.

Funding

This study was supported by the Israel Science Foundation (ISF) (grant No. 2220/22), the Ministry of Health of Israel (grant No. 3-19884for PainSociOT), the German Research Foundation (DFG) (SH 752/2-1), the Congressionally Directed Medical Research Programs (CDMRP) (grant No. AR210005), the United States-Israel Binational Science Foundation (grant No. 2019186) and the HORIZON EUROPE European Research Council (ERC-SyG oxytocINspace).

Supplemental Information

Table S1. An Excel file containing details of all statistical analyses, organized by figure.

Table S2. An Excel file containing processed datasets analyzed and organized by figure.

Tables S3. Contains optogenetic stimulation parameters and data retention rate.

Methods

Resource availability

Further information and requests for resources and reagents should be directed to and will be fulfilled by Shlomo Wagner (shlomow@research.haifa.ac.il).

Materials availability

This study did not generate new unique reagents.

Data and code availability

All the data generated from experiments and the custom codes used to evaluate the conclusions of this paper would be uploaded onto a public repository upon acceptance of the paper.

Main-text figure legends

Figure 1. Behavioral Analysis across four social discrimination tasks.

A. Schematic representation of the SP task.

B. Mean time (±SEM) dedicated by subject mice (n=49 sessions from 21 animals) for investigating the animal stimulus (dark blue) or the object (light blue), and mean sum of transitional bouts between the two stimuli (±SEM, gray lines) across the 5-min encounter period of the SP task in (1-min bins).

C. Median (in box plot) value of mean investigation time of i the social stimulus and the object. Each grey line connects data points of the two stimuli from the same session.

D. Median (in box plot) value of mean duration of all investigation bouts toward the social stimulus and the object.

E. Median (in box plot*) value of the number of non-transitional bouts with the social stimulus and the object.

F-J. As in **A-E**, for the SxP task (n=40 sessions).

K-O. As in **A-E**, for the ESPs task (n=30 sessions).

P-T. As in **A-E**, for the SvF task (n=35 sessions).

***p<0.001, paired samples t-test in **C**, **H**, **M** and **R**.

*$p<0.05$, **p<0.01, ***p<0.001, Wilcoxon signed-rank test in **D-E**, **I-J**, **N-O**, and **S-T**.

Box plot represents 25 to 75 percentiles of the distribution, while the bold line is the median of the distribution. Whiskers represent the smallest and largest values in the distribution.

Figure 2. mPFC pyramidal neurons display context-dependent calcium dynamics during transitional and non-transitional bouts.

A. On the left, a schematic representation of the GCaMP6-expressing AAV vector injection followed by optic fiber implant in the mPFC. On the right, a fluorescent micrograph of an AAV vector-infected mPFC slice, showing GCaMP6-expression (green) and optic fiber location (dashed line).

B. Timeline for a typical session of behavioral testing with fiber photometry recording.

C. Heat-map (see color code to the right of **F**) of the z-scored calcium signals at the beginning (first six seconds) of bout, averaged across all transitional bouts toward the stimulus animals, shown for all sessions of the SP task (n=49 sessions, with each row corresponding to a single session), using 0.5 s bins. Time' 0' represents the beginning of bout.

D-F. As in **C** for the female (SxP; n=40), stressed (ESPs; n=30), and social (SvF; n=35) stimuli, respectively.

G-J. As in **C** for the non-preferred stimuli across the various tasks.

K. Superimposed traces of the mean (±SEM) z-scored calcium signals shown in **C and G**, averaged across all SP sessions. The dark blue and light blue trace lines represent the z-scored calcium signals in transitional bouts to the social stimulus and the object, respectively, during the encounter stage of the SP sessions. Dashed black trace is for transitional bouts to empty chambers during the pre-encounter stage. Blue-shaded areas represent two distinct time windows of the event, which are used for statistical Analysis. Asterisks, representing statistical comparisons between the stimuli and across time windows, are color-coded according to the type of comparison at the top of the graph. Blue and light blue asterisks represent a significant difference in social and object z-scored signals, respectively, during the specific time window relative to baseline. Black asterisks on dashed lines represent a difference in responses to the two stimuli during the same time window. Asterisks on the right side of the graph represent statistical differences for social and object z-scored signals in the encounter stage of the session, during the 3-6 s time window, relative to the pre-encounter stage, and are color-coded according to the stimulus with the significant difference. A significant effect was found for stimulus ($p<0.001$), time ($p<0.001$), and their interaction ($p<0.001$) by two-way MM ANOVA.

L-N. As in **K**, for transitional bouts in the SxP, ESPS, and SvF tasks, respectively. In all three tasks, a significant effect was found for stimulus ($p<0.05$, $p<0.01$, $p<0.001$, respectively),

time (*p<0.001*), and their interaction (*p<0.01* in SxP and ESPs*; p<0.001* in SvF) by two-way MM ANOVA.

O-R. As in **K**, for non-transitional bouts in the SP, SxP, ESPs, and SvF tasks, respectively. A significant effect was found for time (*p<0.01* in SP, *p<0.001* in SxP, *p<0.01* in ESPs, and *p<0.05* in SvF) by two-way MM ANOVA.

Q. Mean trace for the z-scored activity during all transitional bouts from the pooled sessions of the four tasks during the pre-encounter stage (in black), transitional bouts to the preferred stimulus (in blue), and transitional bouts to the non-preferred stimulus (in orange). Please note the difference between the inhibitory response in the trace for transitional bouts to the preferred stimulus, compared to the traces for transitional bouts in the pre-encounter stage and to the less-preferred stimulus.

**p*<0.05, ***p*<0.01, ****p*<0.001, *post-hoc* paired (within stimulus differences in time) or independent (differences between stimuli within time windows, or differences between pre-encounter and encounter) t-test with Holm-Šídák correction for multiple comparisons following detection of main effects by ANOVA.

Figure 3. mPFC pyramidal neurons' activity tracks relative stimulus preference across contexts and internal motivational states.

A. Median relative discrimination index (RDI) for the common stimulus in each of the four tasks. A significant effect was found for task (*p<0.001*) by one-way ANOVA.

B. Heat-map (see color code to the right of **C**) of the average z-scored calcium signals at the beginning (first six seconds) of transitional bouts to the common stimulus, using 0.5-s bins. Time' 0' represents the beginning of the bout. Each line corresponds to a single session in which the common stimulus was the preferred stimulus (RDI > 0), pooled from all four tasks.

C. As in **B**, for transitional bouts to the common stimulus in sessions where it was the non-preferred stimulus (RDI<0), pooled from all four tasks.

D. Superimposed traces of the mean (±SEM) z-scored calcium signals shown in **B-C**, averaged across all sessions. Gray-shaded areas represent three distinct time windows of the event, which were used for the statistical Analysis. A significant effect was found for stimulus (*p<0.001*), time (*p<0.001*), and their interaction (*p<0.001*) by two-way MM ANOVA.

E. Median z-score of the calcium signal during non-transitional bouts to the common stimulus in each of the four tasks, divided into two time windows: -1-to-2 s and 3-to-6 s relative to the bout onset. A significant effect was found for the time effect (*p<0.*001) by two-way MM ANOVA.

F. As in **E**, for transitional bouts. A significant effect was found for stimulus (*p<0.001*), time (*p<0.001*), and their interaction (*p<0.001*) by two-way MM ANOVA.

G. Schematic representation of the SvF task following 24 hours of food deprivation.

H. Median time dedicated by subject animals to investigate the social stimulus (in purple) and the food (in brow, n=24 sessions) during the 5-min encounter period of the SvF-food deprivation task. Each grey line connects data points of the same session.

I. Median sum of non-transitional bouts to the social stimulus and the food during the 5-minute encounter period of the task.

J. Median relative discrimination index (RDI) during the 5-min encounter period of the two conditions of the SvF tasks (satiety and food deprivation).

K. Heat-map (see color code to the right of **L**) of the z-scored calcium signals at the beginning (first six seconds) of non-transitional bouts, averaged across all non-transitional bouts to the social stimulus during the 5-minute encounter stage of all sessions of the SvF-food deprivation task.

L. As in **K**, for non-transitional bouts to the food.

M. Superimposed traces of the mean (±SEM) z-scored calcium signals shown in **K-L,** averaged across all SvF-food deprivation sessions. Paige-shaded areas represent two distinct time windows of the event, which are used for the statistical Analysis. A significant effect was found for stimulus (*p<0.01*) by two-way MM ANOVA.

N-P. As in **K-M**, for transitional bouts. A significant effect was found for stimulus (*p<0.05*), time (*p<0.001*), and their interaction (*p<0.05*) by two-way MM ANOVA.

Q. Superimposed traces of the mean (±SEM) z-scored calcium signals for transitional bouts to the social stimulus in the two conditions of the SvF task.

R. As in **Q**, for transitional bouts to the food.

****p<0.001*, *post-hoc* pairwise comparisons with Holm-Šídák correction following detection of main effects by ANOVA in **A**.

p<0.05*, ***p*<0.01, ****p*<0.001, *post-hoc* paired (within stimulus differences in time) or independent (differences between stimuli within time windows) t-test with Holm-Šídák correction for multiple comparisons following detection of main effects by ANOVA in **D-F, **M** and **P**.

p<0.05*, ***p*<0.01, independent t-test with Holm-Šídák correction for multiple comparisons in **Q-R.

Figure 4. Negative calcium transients in mPFC pyramidal neurons' activity predict social investigation behavior.

A. Heat-map (see color code to the right) of the z-scored social stimulus investigation probability following (4 seconds in 0.2 s bins) the onset of negative change events in the

calcium signal (time '0'), averaged across all negative events within each session, with each row representing one session of the SP task.

B. Superimposed traces of the mean (±SEM) social stimulus investigation probability for 4 seconds following the onset (time '0') of negative change events identified in the pre-encounter stage (black dashed line) and in the encounter stage (dark blue filled line), z-scored to the probability in the -4 to 0 s window in 0.2 s bins, and averaged across all SP sessions.

C-D. As in **A-B**, for the object in SP sessions.

E-H. As in **A-D**, for the SxP task.

I-L. As in **A-D**, for the ESPs task.

M-P. As in **A-D**, for the SvF task.

Q. Mean traces for the investigation probability of the preferred stimulus (in blue) and the non-preferred stimulus (in orange) following negative change events in the calcium signal during the encounter stage of all sessions of the four tasks. Dashed traces represent the investigation probability of empty chambers in the pre-encounter stage, later used to house the preferred and non-preferred stimuli. Please note the high probability of investigating the preferred stimulus in the encounter stage compared to the other traces.

R. As in **Q**, for positive change events.

*$p<0.05$, **$p<0.01$, ***$p<0.001$, One-sample Wilcoxon signed rank test (within trace differences in time) or Wilcoxon signed rank test (differences between pre-encounter and encounter).

Figure 5. Optogenetic activation of mPFC pyramidal neurons modulates social preference.

A. On the left, A schematic representation of the ChR2-expressing AAV vector injection followed by optic fiber implantation in the mPFC. On the left, a fluorescent micrograph of an infected mPFC slice, showing ChR2-mCherry expression (red) and the position of the optic fiber (dashed line).

B. A session example for the investigation times of stimulus 1 (in green), stimulus 2 (in red), and periods of optic stimulation delivered during investigation bouts with stimulus 2 (in blue), across the 5-min duration of the session. The highlighted gray square represents an example bout with stimulus 2 in which optic stimulation (10 ms pulses at 10 Hz frequency) was delivered at the onset of the bout (when the subject's nose touches the mesh of the stimulus chamber) and terminated at the end of the bout (when the subject turns away from the stimulus chamber)

N. Median investigation time of the social (dark blue) and object (light blue) stimuli (n=14), in SP sessions with no stimulation, or when optogenetic stimulation was consistently applied during investigation bouts with the social stimulus, or during investigation bouts

with the object. A significant effect was found for stimulus (*p<0.001*), condition (*p<0.05*), and their interaction (*p<0.001*) by two-way RM ANOVA.

C. Superimposed traces of the normalized mean (±SEM) probability for investigating the social stimulus 6 seconds, in 0.2 s bins, following the bout onset (optic stimulation onset) in SP sessions with no optic stimulation (in gray), and in SP sessions with optic stimulation delivered during bouts with the social stimulus (in dark blue). The gray-shaded area represents the time window (0 to 4 s) taken for statistical Analysis.

D. As in D, for the object stimulus in SP sessions with no optic stimulation (in gray), and in SP sessions with optic stimulation delivered during bouts with the object (in light blue).

E. Median sum of non-transitional bouts to the social stimulus and the object across the three optic stimulation conditions of the SP task.

F. Median logarithmic ratio of non-transitional/transitional bouts for the social stimulus and the object across the three optic stimulation conditions of the SP task. The statistics shown in the figure were calculated from the original data, which was transformed into logarithmic values for graphical convenience due to the significant variation in the original data. A significant effect was found for condition by Kruskal-Wallis test for Social (*p<0.001*) and object (*p<0.01*).

H-L. As in **C-G**, for the SxP task.

M-Q. As in **C-G**, for the ESPs task.

R-V. As in **C-G**, for the SvF task.

W. Median ratio of non-transitional/all bouts for the preferred and the non-preferred stimuli, pulled from all four tasks across the three optic stimulation conditions (no stimulation, stimulation with the preferred stimulus, and stimulation with the non-preferred stimulus). Please note the significant increase in the non-transitional/alll bouts ratio for the stimulus coupled with the optic stimulation.

X. Schematic representation of the behavioral sequence observed during optogenetic stimulation pyramidal neurons in the mPFC. (1) A subject mouse implanted with an optic fiber investigates a stimulus mouse positioned behind a wire mesh barrier. Both animals display engaged social interaction. (2) Blue light stimulation is delivered to the subject mouse, activating mPFC pyramidal neurons at the onset of the investigation bout with the stimulus. (3) The subject mouse exhibits an immediate avoidance response and abruptly ceases interacting with the stimulus. (4) Following the end of investigation bout, and optic stimulation is terminated. (5) Once the optogenetic stimulation ceases, the subject mouse displays renewed motivation to investigate the stimulus. The subject mouse then promptly returns to the mesh barrier to resume investigation of the same stimulus, demonstrating a non-transitional investigation bout.

*$p<0.05$, **$p<0.01$, ***$p<0.001$, *post-hoc* paired t-test with Holm-Šídák correction following detection of main effects by RM ANOVA in **H**, **M**, and **R**.

*$p<0.05$, **$p<0.01$, independent test in **D-E**, **I-J, N-O,** and **S-T**.

*$p<0.05$, **$p<0.01$, independent t-test with Holm-Šídák correction for multiple comparisons in **Q-R**.

*$p<0.05$, **$p<0.01$, ***$p<0.001$, Wilcoxon signed rank test with Holm-Šídák correction for multiple comparisons in **F**, **K**, **P**, and **U**.

*$p<0.05$, **$p<0.01$, ***$p<0.001$, *post-hoc* pairwise comparisons with Holm-Šídák correction for multiple comparisons following detection of main effects by Kruskal-Wallis test in **G**, **L**, **Q**, and **V-W**.

Figure 6. Projection-specific calcium dynamics in mPFC-to-NAc and mPFC-to-BLA neurons during transitional bouts.

A. A schematic representation of the CAV_Cre and mCherry expressing AAV vectors injection into the NAc, and the GCaMP7f AAV vector injection into the mPFC, followed by optic fiber implantation in the mPFC. On the left, a fluorescent micrograph of an infected mPFC slice, showing mCherry (red) and GCaMP7f (green) and the position of the optic fiber (dashed line). On the right, a fluorescent micrograph of an infected NAc slice, showing mCherry (red) expression.

B. As in **A**, for the injection and expression of GCaMP in mPFC-to-BLA projecting neurons.

C. Median investigation time of the social stimulus and the object (n=27 sessions from 11 animals) during the 5-min encounter period of SP sessions recorded from animals with GCaMP expression in mPFC-to-NAc neuronal cells.

D. Superimposed traces of the mean (±SEM) z-scored calcium signals for transitional bouts with the social stimulus (dark blue) and object (light blue), averaged across all SP sessions, and aligned to the bout onset (time '0'). Blue-shaded areas represent two distinct time windows of the event, which were used for the statistical Analysis. A significant effect was found for stimulus ($p<0.01$) and time x stimulus interaction ($p<0.01$) by two-way MM ANOVA.

E-F. As **B-D**, for SP sessions recorded from animals with GCaMP expression in mPFC-to-BLA neuronal cells (n=25 sessions from 12 animals).

G-J. As in **C-F**, for the SxP task ($n_{mPFC\text{-}to\text{-}NAc}=19$; $n_{mPFC\text{-}to\text{-}BLA}=31$).

K-N. As in **C-F**, for the ESPs task ($n_{mPFC\text{-}to\text{-}NAc}=22$; $n_{mPFC\text{-}to\text{-}BLA}=27$).

O-R. As in **C-F**, for the SvF task ($n_{mPFC\text{-}to\text{-}NAc}=18$; $n_{mPFC\text{-}to\text{-}BLA}=32$).

*$p<0.05$, ***$p<0.001$, paired t-test in **C**, **E**, **G**, **I**, **K,** and **M**.

STAR Methods

Method details

Experimental model and subject details

Animals

C57BL/6J: C57BL/6J naïve adult (8-18 week-old) male and female mice (Envigo RMS, Israel) were used either as subjects or stimuli.

Maintenance: Animals were housed in groups of 2-5 sex-matched mice per cage. All behavioral sessions were conducted while subjects were group-housed, with the exception of the SP task in CaMKIIα–GCaMP6f–injected mice, which were recorded after two to three weeks of individual housing to enhance social motivation. All animals were housed at the animal facility of the University of Haifa under veterinary supervision, in a 12 h light/12 h dark cycle (lights on at 9 PM), with *ad libitum* access to food (standard chow diet, Envigo RMS, Israel) and water.

Institutional review board

All experiments were performed according to the National Institutes of Health guide for the care and use of laboratory animals and approved by the Institutional Animal Care and Use Committee of the University of Haifa.

Experiments

Behavioral experiments were conducted in the dark phase of the dark/light cycle in a sound attenuated chamber (Faraday cage), under dim red light.

Experimental setups

The experimental setup [43] consisted of a white Plexiglas arena (37 X 22 X 35 cm) placed in the middle of an acoustic cabinet (60 X 65 X 80 cm). Two Plexiglas triangular chambers (12 cm isosceles, 35 cm height), into which an animal or object (plastic toy) stimulus could be introduced, were placed in two randomly selected opposite corners of the arena. A metal mesh (12 X 6 cm, 1 X 1 cm holes) placed at the bottom of the

triangular chamber allowed direct interaction with the stimulus through the mesh. A high-quality monochromatic camera (Flea3 USB3, Flir for optogenetic experiments or Grasshopper3 for fiber photometry recordings) equipped with a wide-angle lens was placed at the top of the acoustic chamber and connected to a computer, enabling a clear view and recording (~30 frames/s) of subject behavior using commercial software (FlyCapture2 or SpinView, FLIR).

Behavioral paradigms

All behavioral paradigms started with 15 minutes of habituation in which subject animals were moved into the experimental arena with two empty stimuli chambers. Throughout this time, social stimuli were placed in their chambers near the acoustic cabinet for acclimation. After habituation, the chambers containing the relevant stimuli were diagonally placed at opposite ends of the arena in a random fashion. Each task was conducted for 5 minutes, and differed mainly in the stimuli presented to the subjects-

<u>Social preference (SP)</u>: Subject mice were introduced to either a social (naïve, novel, age- and sex-matched conspecific) and an object (mouse-size lego block).

<u>Sex Preference (SxP)</u>: subject mice were presented with a novel male on one side, and a novel female conspecific on the other.

<u>Emotional State Preference for stress stimuli (ESPs)</u> - subject mice were introduced to a naive stimulus animal and to another stimulus animal that had been constrained for 15 min in a 50 ml tube pierced with multiple holes for ventilation. Each "stressed" stimulus animal was used as a stimulus for one session only.

<u>Social vs. food (SvF, in satiety)</u>: Subject mice were introduced to a novel, naïve, social stimulus, and to food pellets composed of standard chow, under satiety conditions (*ad libitum* access to food and water prior to the task). Food pellets were placed inside a dedicated chamber fitted with a metal mesh with small holes (0.5 × 0.5 cm) that prevented subjects from grabbing or consuming the food during testing, thereby minimizing distraction and maintaining engagement with the experimental task.

<u>Social vs. food (SvF, in food deprivation)</u>- subject mice were food deprived, with full access to water for 24 hours before the task. In the task, subjects were introduced to a novel, naïve, social stimulus, and to food pellets composed of standard chow.

Stereotactic surgery for viral injection and optic fiber implantation

Surgery: Mice were anesthetized and analagized with an intraperitoneal injection of a mixture of ketamine, domitor, and the painkiller meloxicam (0.13 mg/g, 0.01 mg/g, and 0.01 mg/g, respectively). Anesthesia levels were monitored by testing toe pinch reflexes and maintained using isoflurane (0.2%; SomnoSuite, Kent Scientific Corporation). Body temperature was kept constant at approximately 37°C using a closed-loop custom-made temperature controller connected to a temperature probe and a heating pad placed under the animal. Ophthalmic ointment (Duratears, Alcon, Couvreur, NV) was applied to maintain eye moisture. Anesthetized animals were fixed in a stereotaxic apparatus (Kopf), with the head flat. The head was shaved, the scalp was disinfected, and the skin was removed to expose the skull. The skull was then leveled using bregma–lambda measurements.

The region of interest was then marked, and a hole (unilateral, right hemisphere) was drilled for viral injection and optic fiber implantation. Additional holes were drilled for supporting screws. Viral injection was performed as previously described in detail (https://star-protocols.cell.com/protocols/1283) using a glass capillary filled with the virus ssAAV-1/2-mCaMK2a-GCaMP6f-WPRE-SV40p(A) for fiber photometry recordings or ssAAV-1/2-mCaMK2α-hChR2(H134R)_mCherry-WPRE-SV40p(A) for excitatory optogenetic stimulation, was slowly lowered into the mPFC (AP, +2 mm; ML, -0.35 mm; DV, +2.0 mm) and left in place for 5 min prior to injection and 10 min following injection to prevent retraction of the virus. For targeting mPFC projecting neurons to the NAc and the BLA, CAV2-Cre (Canine Adenovirus Type 2 expressing Cre recombinase) in combination of 1:5 ratio with ssAAV-1/2-hSyn1-hChR2(H134R)_mCherry-WPRE-hGHp(A) for marking the injection site were injected into either the NAc (AP, +1.42 mm; ML, -1.2 mm; DV, +4.4 mm) or the BLA (AP, -1.43 mm; ML, -3.0 mm; DV, +4.8 mm). ssAAV-1/2-hEF1a-dlox-jGCaMP7f(rev)-dlox-WPRE-bGHp(A) was injected into the mPFC (AP, +2 mm; ML, -0.35 mm; DV, +2.0 mm). The Cav_cre virus was obtained from the Plateforme de Vectorologie de Montpellier (PVM), Institut de Génomique Fonctionnelle, CNRS, University of Montpellier, France. All other viruses were purchased from the Viral Vector Facility (VVF), Institute of Pharmacology & Toxicology, University of Zurich, Switzerland.

A total of 300 nl of the relevant virus was then delivered by manual application using a 50 ml syringe connected to the glass capillary through a plastic tube for applying air pressure (BRAND, disposable BLAUBRAND micropipettes, intraMark, 5 μl). Following

viral injection, an optic fiber (Doric lenses, 200 µm, NA 0.66, 3 mm long, zirconia ferrule, flat-fiber tip) was inserted into the mPFC with the exact coordinates as the viral injection, and placed 200 μm above the injection depth. Screws and optic fiber were fixed to the skull plate using dental cement (UNIFAST, GC America).

After the surgery, antisedan (0.1 mL/10g body weight) was administered subcutaneously to wake the mice from anesthesia. The mice were injected with meloxicam (5%, 0.01 mg/g) and baytril (5%, 0.03 ml/10g) to relieve pain and prevent infections for three days following surgery. Behavioral testing with optogenetic stimulation or fiber photometry was conducted three weeks after surgery to allow optimal viral expression. Following surgery, all subjects were housed with one or two cage mates.

***In vivo* fiber photometry recordings**

Test: All fiber photometry recordings were performed using the apparatus described above. The optic fiber of the implanted mouse was connected to the optical patch cords via a sleeve connector (Doric) under brief isoflurane anesthesia. The wired animal was then allowed to habituate in the behavior setup for 15 min. The recording session started with an additional 5-minute baseline (pre-encounter) period with empty chambers. Thereafter, the empty chambers were replaced with chambers containing the appropriate stimuli for a 5-minute test. Following the test, the stimulus-containing chambers were again replaced with empty ones for an additional 5 minutes. Each subject was recorded in two different task sessions per day, with at least 40 minutes between sessions for the same animal.

Fiber photometry recording and synchronization: Calcium signals were recorded using one of two fiber photometry recording setups composed of the RZ10x system of Tucker Davis Technologies and an optical path by Doric, which includes 600 µm mono-fiber optic patch cords connected to either a four ports Fluorescence MiniCube (FMC4_IE(400-410)_E(460-490)_F(500-550)_S) for one-color recordings or a six ports Fluorescence MiniCube (FMC6_IE(400-410)_E1(460-490)_F1(500-540)_E2(555-570)_F2(580-680)_S) for two-colors recordings. Optic paths were connected using a 200 µm optical patch cord with a fiber-optic rotary joint (FRJ_1×1_PT_200/230/LWMJ-0.57_1m_FCM_0.15m_FCM) that was connected to the recorded animal. A camera (Grasshopper3 USB3, FLIR) was placed on top of the arena and connected to the digital

port of the RZ10× system and configured to deliver strobes for every frame acquired at a frame rate of 30 frames/sec. These were later used to synchronize the video frames with the calcium signal. TDT Synapse software was used to record the GCaMP6f/7f signal channel (excitation at 465 nm, modulated at 330 Hz), the isosbestic control channel (405 nm, modulated at 210 Hz), and the digital channel receiving the camera strobes, with a sampling rate of ~10^17.3 Hz. LED currents were adjusted to return the voltage to between 0 and 200 mV for each signal, were offset by 5 mA, and were demodulated using a 6 Hz low-pass frequency filter. Light intensity levels for the 465-nm and 405-nm channels were verified by measuring output power with an external power meter (PM100D, Thorlabs) every 2–3 recording days.

***In vivo* optogenetic stimulation**

Test: In all optogenetic experiments (SP, SxP, ESPs, SvF–Satiety, and SvF–Food Deprivation), subject mice (n = 14) were connected to the stimulation apparatus and allowed to habituate for 20 min in an arena containing empty chambers. After habituation, the empty chambers were replaced with the appropriate stimuli, and interactions were recorded for 5 min. In control experiments with empty chambers, new empty chambers were introduced into the arena at this stage.

Each subject was tested three times in the SP, SxP, ESPs, and SvF tasks, each session employing a different stimulation condition: (1) no stimulation, (2) stimulation delivered during investigation bouts with one of the two presented stimuli, and (3) stimulation delivered during investigation bouts with the other stimulus. Optic stimulation during an investigation bout was manually delivered and defined as light delivery from the onset of nose contact with the mesh of a stimulus chamber until the subject's head turned away from it.

In the SvF–Food Deprivation and empty-chambers tasks, each mouse was tested twice—once without stimulation and once with optic stimulation delivered during investigation bouts with either the social stimulus (SvF–Food Deprivation) or one of the empty chambers.

Each day, subject mice participated in either a single experiment with optogenetic stimulation or in two sequential experiments, consisting of a non-stimulated session followed 20 minutes later by a stimulated session. In the SvF–Food Deprivation task, both conditions were conducted on the same day, with the non-stimulated session

always preceding the stimulated session, to avoid repeated food-deprivation manipulations. All other tasks were conducted in a randomized order.

Optogenetic stimulation: Subject mice were lightly anesthetized with isoflurane and connected to the laser (473 nm, model FTEC2471-M75YY0, Blue Sky Research) via a fiber-optic rotary joint attached to 200 µm core multimode fiber patch cables connecting the animal to the light source for optic stimulation delivery (Thorlabs, Fiber Optic Rotary Joint Patch Cables for Optogenetics, product group #6865). Animals were given 20 min to recover from any residual effects of the brief isoflurane anesthesia before testing, until they showed full mobility. In all experiments, optogenetic stimulation consisted of continuous light pulses delivered at 10 Hz throughout the entire duration of each investigation bout with a given stimulus. The initial photo-stimulation protocol used 10 ms pulses at a light power of 8.23 mW. However, these parameters induced seizure-like behavior in a subset of animals, which we attributed to the high level of ChR2 expression in the mPFC. This phenomenon has been previously reported in optogenetic studies of cortical regions, where brief optogenetic stimuli can elicit seizures that increase in severity with repeated stimulation (Cela et al., 2019; Osawa et al., 2013). To ensure that experimental outcomes reflected controlled neuronal modulation rather than pathological network states, we systematically optimized the stimulation parameters by first reducing light power from 8.23 mW to no lower than 4.65 mW, and subsequently shortening pulse duration from 10 ms to 7 ms, while maintaining the 10 Hz frequency (see Tables S3A-B for detailed timeline and voltage-light power calibration). The minimal used parameters of 4.65 mW and 7 ms pulses are well within the established range for effective ChR2 activation in vivo. Using a computational model based on direct measurements in mammalian brain tissue [44] (https://web.stanford.edu/group/dlab/cgi-bin/graph/chart.php), we calculated that 4.65mW of 473nm light delivered through a 200µm fiber (NA 0.66) produces an irradiance of approximately 4.99mW/mm² at 250µm distance from the fiber tip (the maximal distance between the fiber tip and the virus injection site), and 1.26mW/mm^2 at a distance of 500µm which is the highest penetration depth of blue light stimulation in rodent brain tissues [36]. These values exceed the generally accepted threshold of 1 mW/mm² required for suprathreshold activation of ChR2-expressing neurons [44-46], while remaining within the recommended safe operating range of less than 10-20 mW/mm² at target cells to minimize tissue heating [36]. Furthermore, our pulse duration of 7 ms is well above the opening rate time

constant of ChR2 ($\tau \approx 1.21$ ms), ensuring sufficient channel opening to trigger action potentials reliably [3-Lin 2011]. Optical stimulation was manually delivered via a Master8 Channel Programmable Pulse Stimulator (A.M.P.I). Sessions in which severe seizures prevented completion of behavioral testing were excluded from analysis. Overall, 12 out of 150 stimulation sessions (8%) were excluded due to severe seizures, yielding a 92% data retention rate across all animals (Table S3C). Importantly, even at the optimized parameters (4.65 mW, 7 ms pulses, 10 Hz), animals continued to exhibit the intended behavioral response pattern, characterized by abrupt termination of investigation bouts upon stimulation onset, followed by immediate re-engagement with the same stimulus once stimulation ceased, confirming that the optimized parameters were sufficient to produce the desired modulatory effect on mPFC pyramidal neuron activity. Importantly, even at the lowest parameters (4.65 mW, 7 ms pulses, 10 Hz), animals continued to exhibit the intended behavioral response pattern, characterized by the abrupt termination of investigation bouts upon stimulation onset, followed by immediate re-engagement with the same stimulus once stimulation ceased (see Supp. Movie 3).

Post-mortem **histological Analysis of viral injections and optic-fiber placement**

Each implanted mouse was anesthetized with isoflurane (induction: 3%, 0.5%-0.8% maintenance in 200 mL/min of air), attached to the stereotaxic device, and the optic fiber implant was gently extracted from its head. The mouse was then perfused with phosphate-buffered saline (PBS) and fixed using a 4% paraformaldehyde (PFA, Sigma) solution. The brains were harvested and placed in PFA (4%) for 48 hours, followed by sectioning into 50-µm slices in the horizontal axis using a VT1200s Leica sliding vibratome. The slices were collected onto microscope slides and stained with DAPI (Fluoroshield with DAPI, histology mounting medium, Merck). Images of subject brain slices were acquired for verification of the viral expression placement and optic fiber path within the mPFC using an epifluorescence microscope (Ti2 eclipse, Nikon) equipped with a blue filter for DAPI staining, FITC for detecting GCaMP6f/7f-expressing cells, and TRITC for detecting mCherry-expressing cells.

Quantification and statistical analysis

All processed data are detailed in Table S2, organized by the various figures.

Tracking software and behavioral analyses

All video recordings were analyzed using *TrackRodent* (https://github.com/shainetser/TrackRodent) [47]. The *BlackMouseWiredBodyBased* algorithm was applied to sessions involving tethered animals in both fiber photometry and optogenetic experiments. Behavioral analyses were performed as previously described [48].

Parameters for behavioral quantification

All behavioral parameters reported in this study were automatically extracted using the TrackRodent software, which continuously tracks the animal's position and investigation of the stimuli chambers throughout the experiment. Behavioral events were identified and quantified using predefined algorithms and rule-based classifications embedded in the software. The Relative Discrimination Index (RDI) was calculated as the difference in investigation time between the two stimuli—specifically, investigation of the preferred stimulus minus the investigation of the non-preferred stimulus—normalized by the total investigation time toward both stimuli. For the naïve male stimulus (the common stimulus across all four tasks), the RDI was calculated as the investigation time for the common stimulus (independent of preference) minus the investigation time for the other stimulus, divided by the sum of both.

Investigation bouts were defined as events beginning when the animal's head (or body center, depending on the selected algorithm in TrackRodent software) made contact with the metal mesh of the stimulus chamber and ending when the animal disengaged from the mesh. Each bout was subsequently categorized as either non-transitional or transitional. Non-transitional bouts were those preceded by a bout directed toward the same stimulus, whereas transitional bouts were those preceded by a bout directed toward the alternate stimulus. A minimum interval of >0.5 s between successive bouts was required to classify bouts as distinct. Behavioral events of interest detected by TrackRodent were then aligned with the calcium imaging data to enable precise synchronization between neural activity and behavior.

Synchronization of physiological data to behavioral events

We used a custom-made code called DeepPhenotyping to visualize and synchronize the different signals and behavioral events, as previously described [49, 50]. For the calcium signal with each event type ("Transitional bouts" and "Non-transitional bouts"), the

software considered the relevant sample rate and aligned the signal to the beginning of the event. For calculating the subjects' investigation probability of a given stimulus between different optic stimulation conditions, the investigation time for the relevant stimulus was synchronized to the onset of all bouts (regardless of type) which is also the onset of the optical stimulation in conditions where optic stimulation was delivered. Derived investigation probabilities were then normalized to the maximum (divided by P_{max} of 1) and used directly for statistical Analysis.

Calcium signal data analysis

Calcium signals were analyzed using DeepPhenotyping. We first fitted the 405 nm channel onto the 465 nm channel to de-trend signal bleaching and any movement artifacts, according to the manufacturer's protocol(https://github.com/tjd2002/tjd-shared-code/blob/master/matlab/photometry/FP_normalize.m). Next, the de-trended signal was aligned to the video recording using the timestamps recorded by the digital port of the RZ10× system. We aligned the de-trended signal to each bout type (transition\non-transition) event and normalized it using the z-score (0.5 s bins), with the pre-event period of -4 s to -1 s serving as a baseline.

As for calculating the population average signal amplitude over time, we first calculated the AUC for each session in time bins of five seconds (using the original detrended signal which is samples at 1017.3Hz) and then averaged the signals across all sessions.

For calculating the probability of social investigation following significant negative or positive changes in calcium activity, we first segmented the GCaMP signal into 0.2-s time bins. For each bin, neural activity was z-scored within an 8-s window (−4 s to +4 s relative to the bin onset) using the preceding 4 s (−4 s to 0 s) as baseline. The mean z-score during the 4 s following each bin was then compared to baseline activity. Time bins showing a significant deviation ($|Z| \geq 1.96$) were classified as either positive or negative calcium events. Following the detection of a positive or negative event, a 6-s interval was imposed before the next sampling bin to ensure that detected events were distinct and did not reflect the same change in the recorded signal at adjacent time points. All identified positive and negative events were subsequently aligned with the animal's investigation time of a given stimulus, and the probability of investigation was calculated in 8-s time windows centered on the event onset. The mean probability during the −4 to 0 s interval served as the baseline for z-scoring post-event (0 to 4 s)

probabilities. z-scored probabilities for positive and negative events were then averaged across all events pooled within each session. The area under the curve (AUC) in the 0-to4s time window was computed to quantify differences in investigation probability following positive versus negative events, as well as to assess deviations from baseline (0) within each event type.

Statistical Analysis

All statistical results and parameters are presented in Table S1, organized according to the corresponding figures. Sample sizes for all behavioral experiments were determined based on previously published power calculations [48]. Statistical analyses were performed using SPSS v27.0 (IBM) and GraphPad Prism v10.1.2 (GraphPad Software). The Kolmogorov–Smirnov and Shapiro–Wilk tests were used to assess the normality of the dependent variables. For normally distributed data, one-sample *t*-tests were used to compare group means to a fixed reference value (0 in this case). Two-tailed paired *t*-tests were used to compare conditions or stimuli within the same group, and two-tailed independent *t*-tests were used to compare variables between distinct groups. When normality assumptions were violated, nonparametric alternatives were applied. The Wilcoxon signed-rank test was used to compare group medians to a set value (0) or between conditions within the same group, and the Mann–Whitney *U* test was used to compare conditions between groups. For comparisons involving multiple factors, analyses of variance (ANOVA) were conducted according to the experimental design. Mixed-model (MM) ANOVA was applied when data included both within-subject (repeated-measures) and between-subject factors. This model included one random effect (subject ID), one within-subject effect, one between-subject effect, and their interaction. Two-way between-subjects ANOVA was used for comparisons between groups involving two independent factors, whereas two-way repeated-measures (RM) ANOVA was used for comparisons within groups across multiple conditions or variables. The latter model included one random effect (subject ID), two within-subject effects, and their interaction. When the assumption of sphericity required for ANOVA was violated, the Greenhouse–Geisser correction was applied. Whenever significant main effects or interactions were detected, post hoc Student's *t*-tests with Holm–Šidák correction were conducted. For repeated-measures data violating normality assumptions, Friedman's nonparametric test was applied, followed by post hoc Dunn's paired comparisons. For between-group comparisons involving more than two levels, the Kruskal–Wallis test was

used, followed by Dunn's multiple-comparisons post hoc tests. Statistical significance was set at $p < 0.05$.

References

1. Chen, P. and W. Hong, *Neural Circuit Mechanisms of Social Behavior.* Neuron, 2018. **98**(1): p. 16-30.
2. Gangopadhyay, P., et al., *Prefrontal–amygdala circuits in social decision-making.* Nature neuroscience, 2021. **24**(1): p. 5-18.
3. Kietzman, H.W. and S.L. Gourley, *How social information impacts action in rodents and humans: the role of the prefrontal cortex and its connections.* Neuroscience & Biobehavioral Reviews, 2023. **147**: p. 105075.
4. Cao, W., H. Li, and J. Luo, *Prefrontal cortical circuits in social behaviors: an overview.* Journal of Zhejiang University-SCIENCE B, 2024. **25**(11): p. 941-955.
5. Bicks, L.K., et al., *Prefrontal Cortex and Social Cognition in Mouse and Man.* Front Psychol, 2015. **6**: p. 1805.
6. Ko, J., *Neuroanatomical Substrates of Rodent Social Behavior: The Medial Prefrontal Cortex and Its Projection Patterns.* Front Neural Circuits, 2017. **11**: p. 41.
7. Lee, E., et al., *Enhanced neuronal activity in the medial prefrontal cortex during social approach behavior.* Journal of Neuroscience, 2016. **36**(26): p. 6926-6936.
8. Yashima, J., T. Uekita, and T. Sakamoto, *The prelimbic cortex but not the anterior cingulate cortex plays an important role in social recognition and social investigation in mice.* PloS one, 2023. **18**(4): p. e0284666.
9. Kuga, N., et al., *Prefrontal-amygdalar oscillations related to social behavior in mice.* eLife, 2022. **11**: p. e78428.
10. Li, H., et al., *Brain circuits that regulate social behavior.* Molecular Psychiatry, 2025: p. 1-17.
11. van den Bos, W. and B. Güroğlu, *The role of the ventral medial prefrontal cortex in social decision making.* Journal of Neuroscience, 2009. **29**(24): p. 7631-7632.
12. Euston, D.R., A.J. Gruber, and B.L. McNaughton, *The role of medial prefrontal cortex in memory and decision making.* Neuron, 2012. **76**(6): p. 1057-1070.
13. Levy, D.R., et al., *Dynamics of social representation in the mouse prefrontal cortex.* Nat Neurosci, 2019. **22**(12): p. 2013-2022.
14. Glanzberg, J.T., et al., *Individual differences in prelimbic neural representation of food and cocaine seeking.* Cell reports, 2024. **43**(12).
15. Frost, N.A., et al., *Context-invariant socioemotional encoding by prefrontal ensembles.* Nature Communications, 2025. **16**(1): p. 5455.
16. Isaac, J., et al., *Sex differences in neural representations of social and nonsocial reward in the medial prefrontal cortex.* Nature Communications, 2024. **15**(1): p. 8018.
17. Lam, N.H., et al., *Effects of altered excitation-inhibition balance on decision making in a cortical circuit model.* Journal of Neuroscience, 2022. **42**(6): p. 1035-1053.

18. Tan, T., et al., *Neural circuits and activity dynamics underlying sex-specific effects of chronic social isolation stress.* Cell Rep, 2021. **34**(12): p. 108874.
19. Huang, W.-C., Y. Chen, and D.T. Page, *Hyperconnectivity of prefrontal cortex to amygdala projections in a mouse model of macrocephaly/autism syndrome.* Nature communications, 2016. **7**(1): p. 13421.
20. Liu, Y., et al., *A molecularly defined mPFC-BLA circuit specifically regulates social novelty preference.* Science Advances, 2025. **11**(17): p. eadt9008.
21. Yizhar, O., et al., *Neocortical excitation/inhibition balance in information processing and social dysfunction.* Nature, 2011. **477**(7363): p. 171-178.
22. Kingsbury, L. and W. Hong, *A multi-brain framework for social interaction.* Trends in neurosciences, 2020. **43**(9): p. 651-666.
23. Klune, C.B., B. Jin, and L.A. DeNardo, *Linking mPFC circuit maturation to the developmental regulation of emotional memory and cognitive flexibility.* Elife, 2021. **10**: p. e64567.
24. Ebstein, R.P., et al., *Genetics of human social behavior.* Neuron, 2010. **65**(6): p. 831-844.
25. McGraw, L.A. and L.J. Young, *The prairie vole: an emerging model organism for understanding the social brain.* Trends in neurosciences, 2010. **33**(2): p. 103-109.
26. Carlén, M., *What constitutes the prefrontal cortex?* Science, 2017. **358**(6362): p. 478-482.
27. Netser, S., et al., *Distinct dynamics of social motivation drive differential social behavior in laboratory rat and mouse strains.* Nat Commun, 2020. **11**(1): p. 5908.
28. Jabarin, R., et al., *Distinct prelimbic cortex neuronal responses to emotional states of others drive emotion recognition in adult mice.* Current Biology, 2025. **35**(5): p. 994-1011. e8.
29. Anastasiades, P.G. and A.G. Carter, *Circuit organization of the rodent medial prefrontal cortex.* Trends in neurosciences, 2021. **44**(7): p. 550-563.
30. Scheggia, D., et al., *Somatostatin interneurons in the prefrontal cortex control affective state discrimination in mice.* Nature neuroscience, 2020. **23**(1): p. 47-60.
31. Sul, J.H., et al., *Distinct roles of rodent orbitofrontal and medial prefrontal cortex in decision making.* Neuron, 2010. **66**(3): p. 449-460.
32. Wang, Q., et al., *Distributed value representation in the medial prefrontal cortex during intertemporal choices.* Journal of Neuroscience, 2014. **34**(22): p. 7522-7530.
33. Gabriel, C.J., et al., *Transformations in prefrontal ensemble activity underlying rapid threat avoidance learning.* Current Biology, 2025. **35**(5): p. 1128-1136. e4.
34. Klavir, O., et al., *Manipulating fear associations via optogenetic modulation of amygdala inputs to prefrontal cortex.* Nature neuroscience, 2017. **20**(6): p. 836-844.
35. Yizhar, O., *Optogenetic insights into social behavior function.* Biological psychiatry, 2012. **71**(12): p. 1075-1080.
36. Yizhar, O., et al., *Optogenetics in neural systems.* Neuron, 2011. **71**(1): p. 9-34.
37. Choi, T.-Y., et al., *Distinct prefrontal projection activity and transcriptional state conversely orchestrate social competition and hierarchy.* Neuron, 2024. **112**(4): p. 611-627. e8.
38. Huang, W.-C., et al., *Social behavior is modulated by valence-encoding mPFC-amygdala sub-circuitry.* Cell reports, 2020. **32**(2).
39. Giustino, T.F. and S. Maren, *The role of the medial prefrontal cortex in the conditioning and extinction of fear.* Frontiers in behavioral neuroscience, 2015. **9**: p. 298.

40. Selimbeyoglu, A., et al., *Modulation of prefrontal cortex excitation/inhibition balance rescues social behavior in CNTNAP2-deficient mice.* Science translational medicine, 2017. **9**(401): p. eaah6733.
41. Luo, Y., et al., *Reduced excitatory activity in the developing mPFC mediates a PVH-to-PVL transition and impaired social cognition in autism spectrum disorders.* Translational Psychiatry, 2024. **14**(1): p. 325.
42. Ferguson, B.R. and W.-J. Gao, *PV interneurons: critical regulators of E/I balance for prefrontal cortex-dependent behavior and psychiatric disorders.* Frontiers in neural circuits, 2018. **12**: p. 37.
43. Netser, S., et al., *A novel system for tracking social preference dynamics in mice reveals sex-and strain-specific characteristics.* Molecular autism, 2017. **8**(1): p. 53.
44. Aravanis, A.M., et al., *An optical neural interface: in vivo control of rodent motor cortex with integrated fiberoptic and optogenetic technology.* Journal of neural engineering, 2007. **4**(3): p. S143.
45. Cela, E., et al., *An optogenetic kindling model of neocortical epilepsy.* Scientific Reports, 2019. **9**(1): p. 5236.
46. Britt, J.P., R.A. McDevitt, and A. Bonci, *Use of channelrhodopsin for activation of CNS neurons.* Current protocols in neuroscience, 2012. **58**(1): p. 2.16. 1-2.16. 19.
47. Netser, S., et al., *A novel system for tracking social preference dynamics in mice reveals sex- and strain-specific characteristics.* Mol Autism, 2017. **8**: p. 53.
48. Netser, S., et al., *A system for tracking the dynamics of social preference behavior in small rodents.* Journal of Visualized Experiments (JoVE), 2019(153): p. e60336.
49. Barbier, M., et al., *Altered Neural Activity in the Mesoaccumbens Pathway Underlies Impaired Social Reward Processing in Shank3-Deficient Rats.* Advanced Science, 2025. **12**(17): p. 2414813.
50. Mohapatra, A.N., et al., *Impaired emotion recognition in Cntnap2-deficient mice is associated with hyper-synchronous prefrontal cortex neuronal activity.* Molecular Psychiatry, 2025. **30**(4): p. 1440-1452.

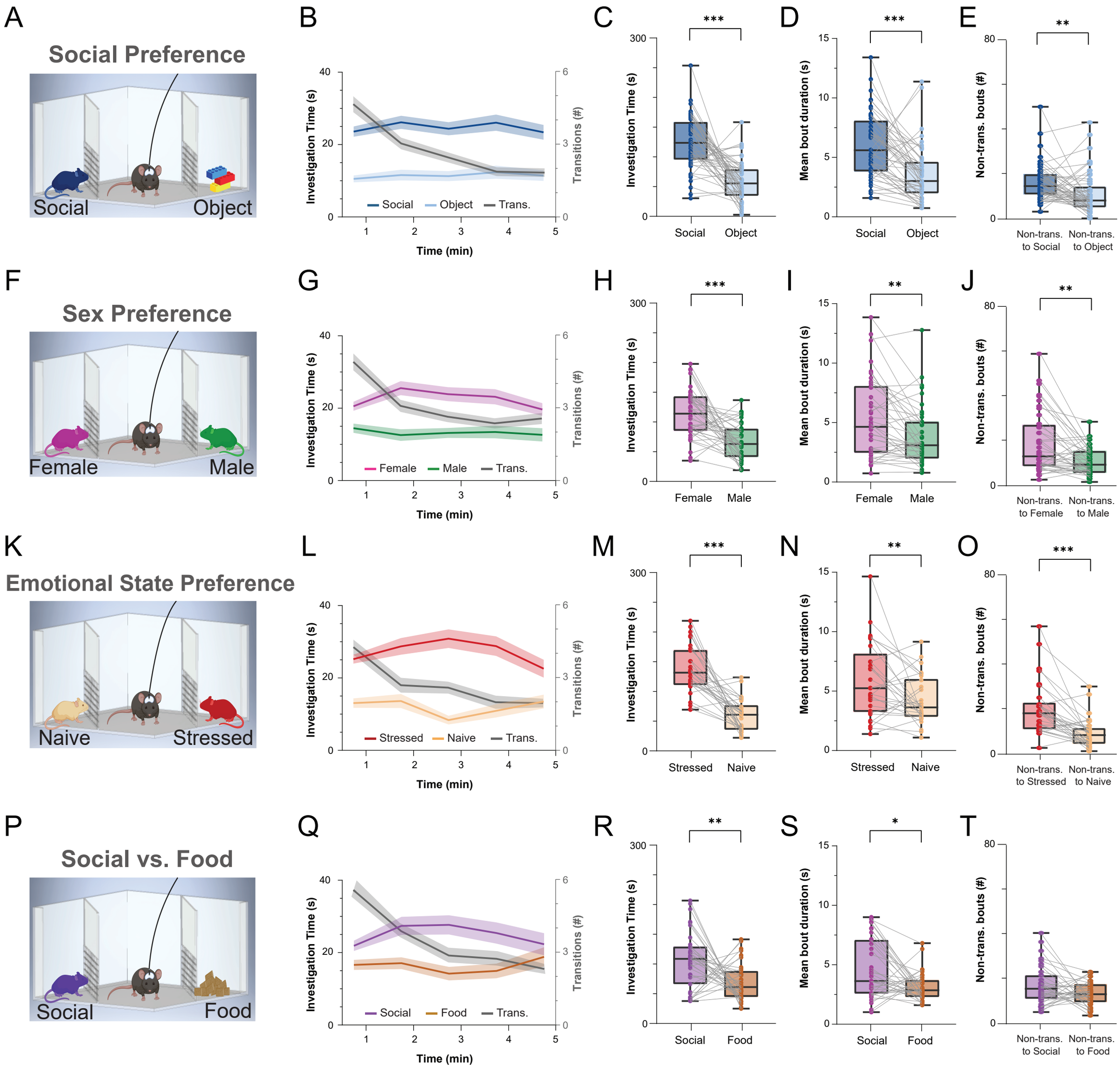
A
Social Preference
Social
Object
B
Investigation Time (s)
Transitions (#)
Time (min)
Social
Object
Trans.
C
Investigation Time (s)
Social
Object
D
Mean bout duration (s)
Social
Object
E
Non-trans. bouts (#)
Non-trans. to Social
Non-trans. to Object
F
Sex Preference
Female
Male
G
Female
Male
Trans.
H
Female
Male
I
Female
Male
J
Non-trans. to Female
Non-trans. to Male
K
Emotional State Preference
Naive
Stressed
L
Stressed
Naive
Trans.
M
Stressed
Naive
N
Stressed
Naive
O
Non-trans. to Stressed
Non-trans. to Naive
P
Social vs. Food
Social
Food
Q
Social
Food
Trans.
R
Social
Food
S
Social
Food
T
Non-trans. to Social
Non-trans. to Food

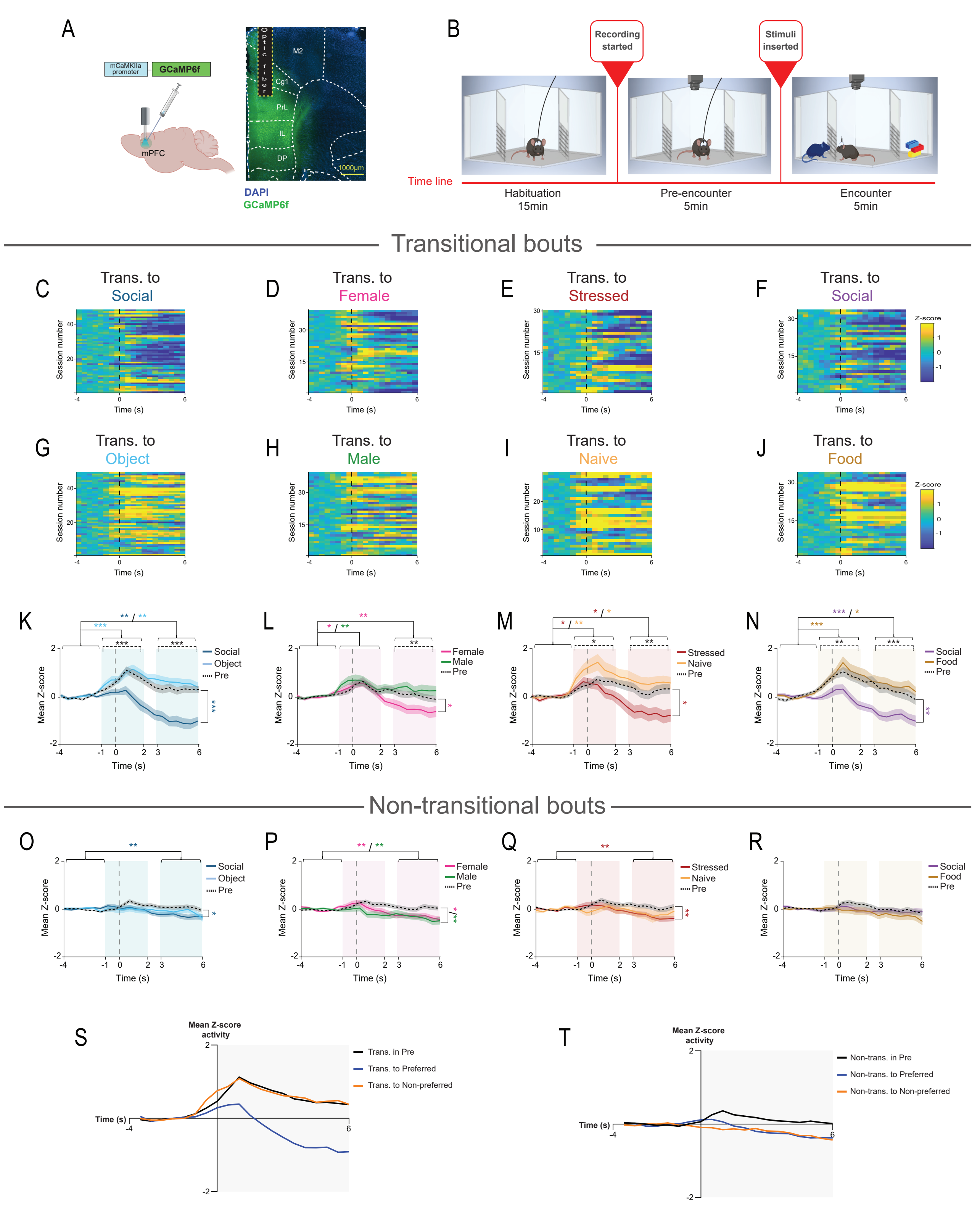
A
mCaMKIIa promoter
GCaMP6f
mPFC
Optic fiber
M2
Cg1
PrL
IL
DP
1000μm
DAPI
GCaMP6f
B
Recording started
Stimuli inserted
Time line
Habituation 15min
Pre-encounter 5min
Encounter 5min
Transitional bouts
C Trans. to Social
D Trans. to Female
E Trans. to Stressed
F Trans. to Social
G Trans. to Object
H Trans. to Male
I Trans. to Naive
J Trans. to Food
Session number
Time (s)
Z-score
K
L
M
N
Mean Z-score
Social
Object
Pre
Female
Male
Stressed
Naive
Food
Non-transitional bouts
O
P
Q
R
S
T
Mean Z-score activity
Trans. in Pre
Trans. to Preferred
Trans. to Non-preferred
Non-trans. in Pre
Non-trans. to Preferred
Non-trans. to Non-preferred

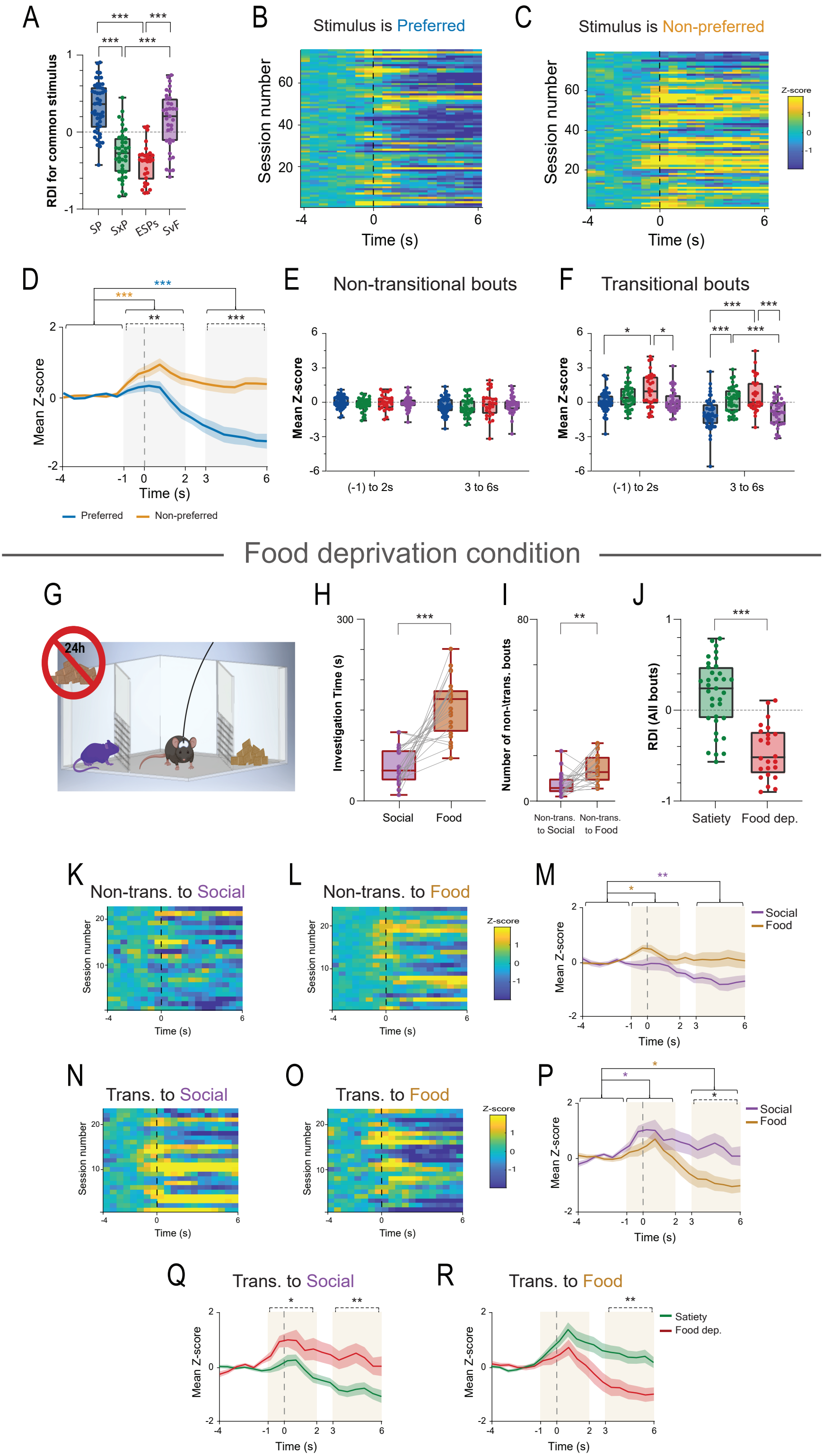
A
RDI for common stimulus
SP
SxP
ESPs
SvF
B
Stimulus is Preferred
Session number
Time (s)
C
Stimulus is Non-preferred
Z-score
D
Mean Z-score
Time (s)
Preferred
Non-preferred
E
Non-transitional bouts
(-1) to 2s
3 to 6s
F
Transitional bouts
Food deprivation condition
G
24h
H
Investigation Time (s)
Social
Food
I
Number of non-trans. bouts
Non-trans. to Social
Non-trans. to Food
J
RDI (All bouts)
Satiety
Food dep.
K
Non-trans. to Social
L
Non-trans. to Food
M
Social
Food
N
Trans. to Social
O
Trans. to Food
P
Q
Trans. to Social
R
Trans. to Food
Satiety
Food dep.

Social Preference

Social

A

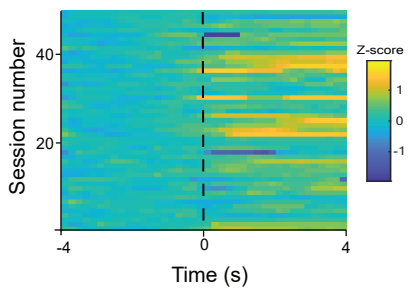

B

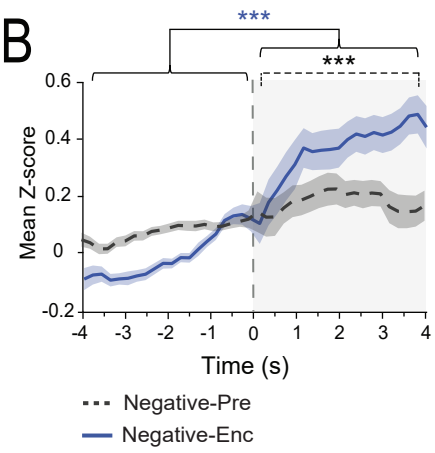

Object

C

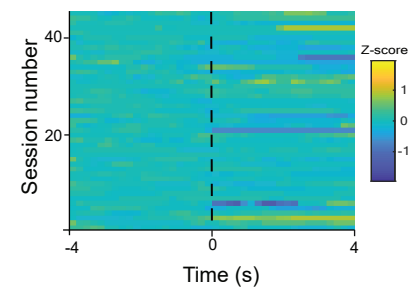

D

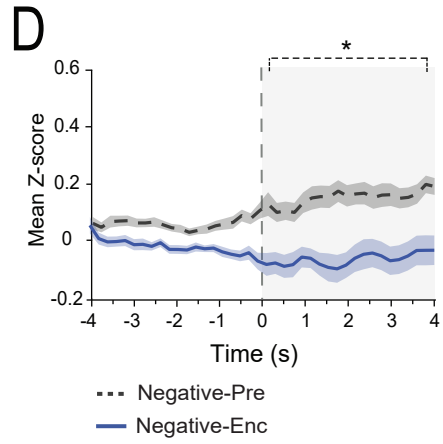

Sex Preference

Female

E

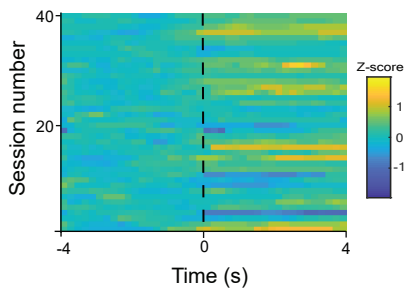

F

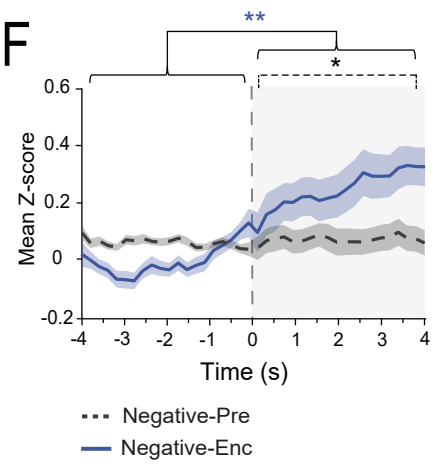

Male

G

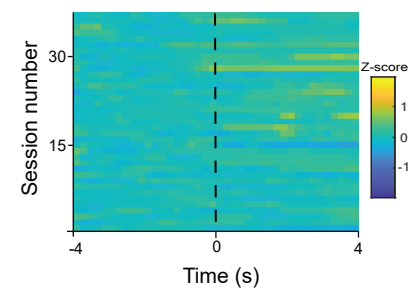

H

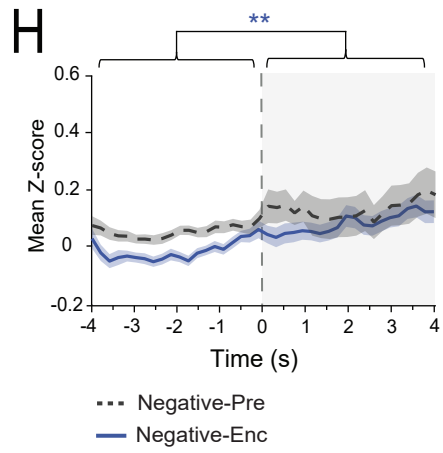

Emotional State Preference-stress

Stressed

I

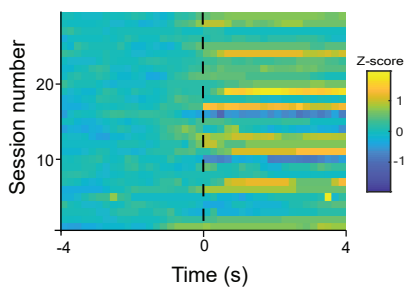

J

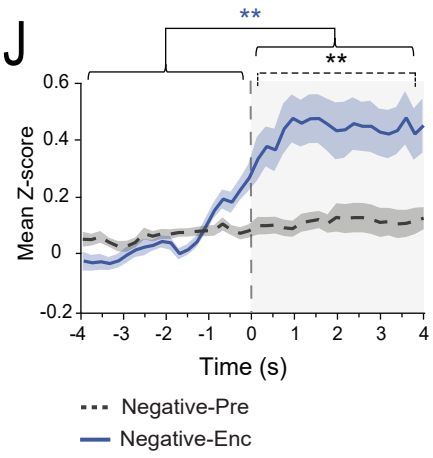

Naive

K

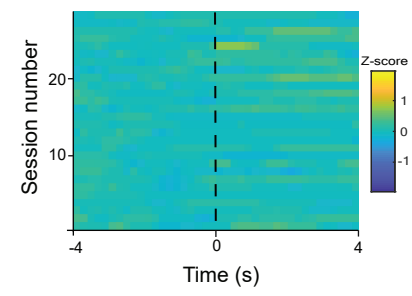

L

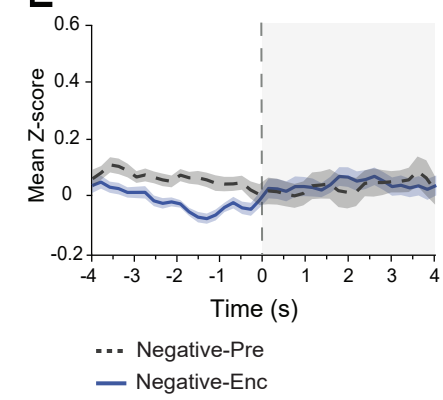

Social vs. Food

Social

M

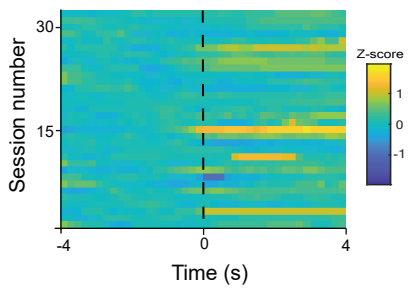

N

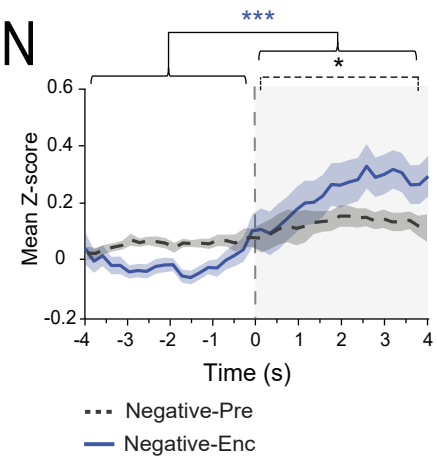

Food

O

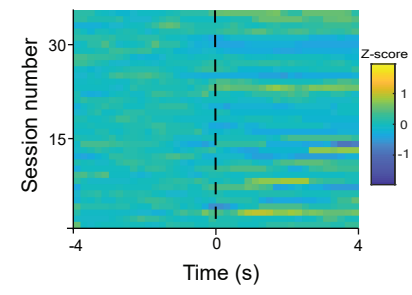

P

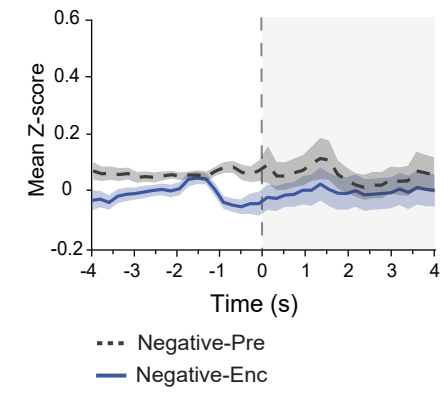

Q

Negative changes

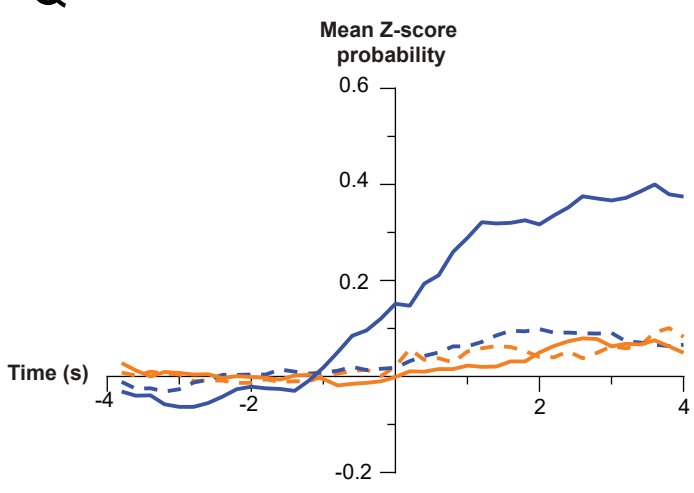

R

Positive changes

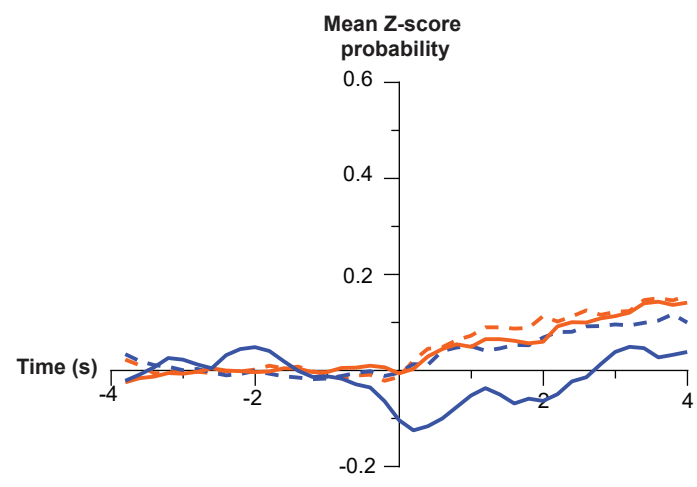

Preferred_Pre
Non-preferred_Pre
Preferred_Enc
Non-preferred_Enc

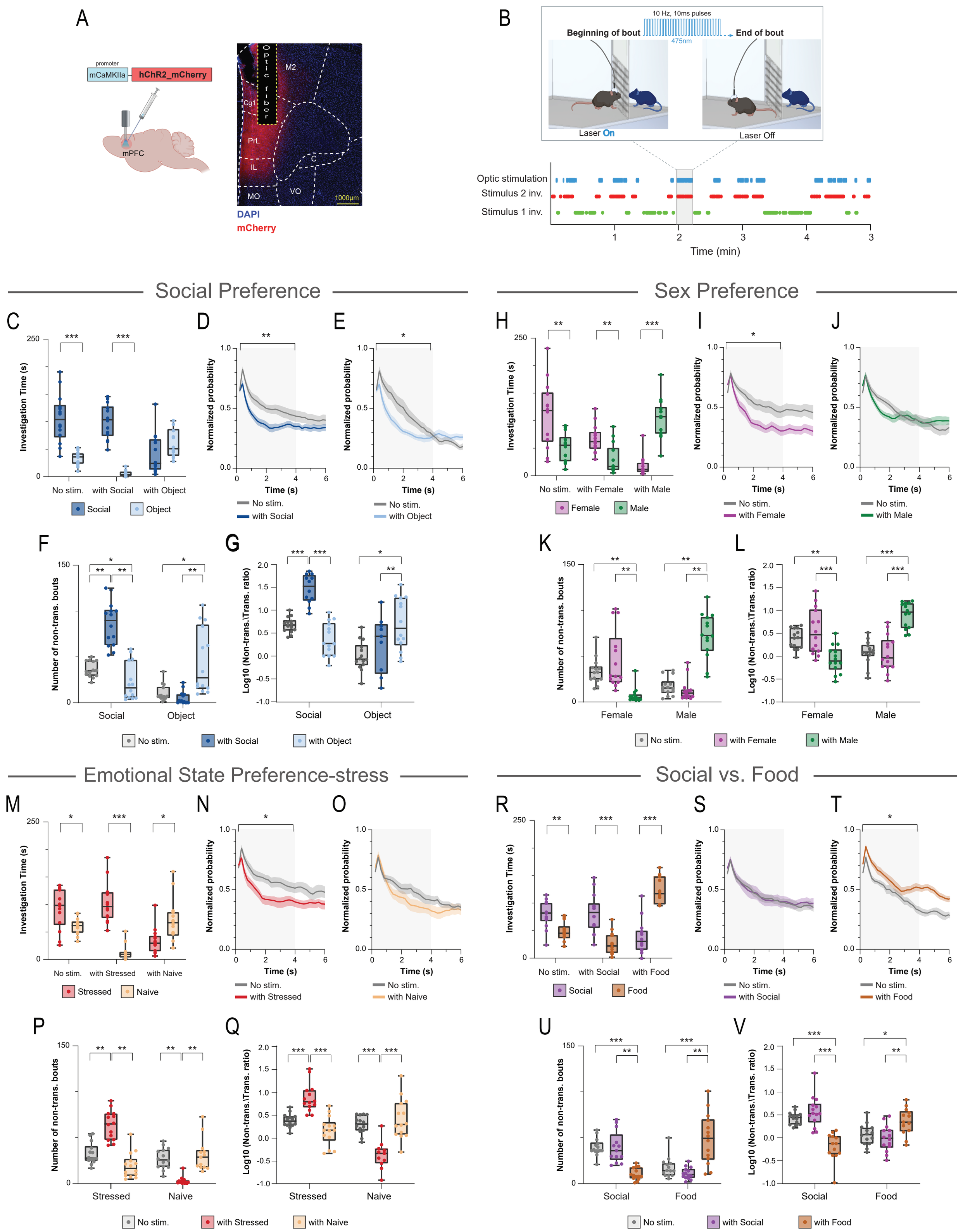
A
promoter
mCaMKIIa
hChR2_mCherry
mPFC
Optic fiber
M2
Cg1
PrL
IL
C
MO
VO
1000µm
DAPI
mCherry
B
10 Hz, 10ms pulses
Beginning of bout
End of bout
475nm
Laser On
Laser Off
Optic stimulation
Stimulus 2 inv.
Stimulus 1 inv.
Time (min)
Social Preference
Sex Preference
Investigation Time (s)
No stim.
with Social
with Object
Social
Object
Normalized probability
Time (s)
with Female
with Male
Female
Male
Number of non-trans. bouts
Log10 (Non-trans.\Trans. ratio)
Emotional State Preference-stress
Social vs. Food
with Stressed
with Naive
Stressed
Naive
with Food
Food
Non-trans\All bouts ratio
with preferred
with non-preferred
Preferred
Non-preferred
Start of an investigation bout
Delivery of optogenetic stimulation
Abrupt termination of interaction
Termination of optic stimulation
Motivation to invesitigate stimulus persists
Return to stimulus "Non-transitional bout"
ON
OFF

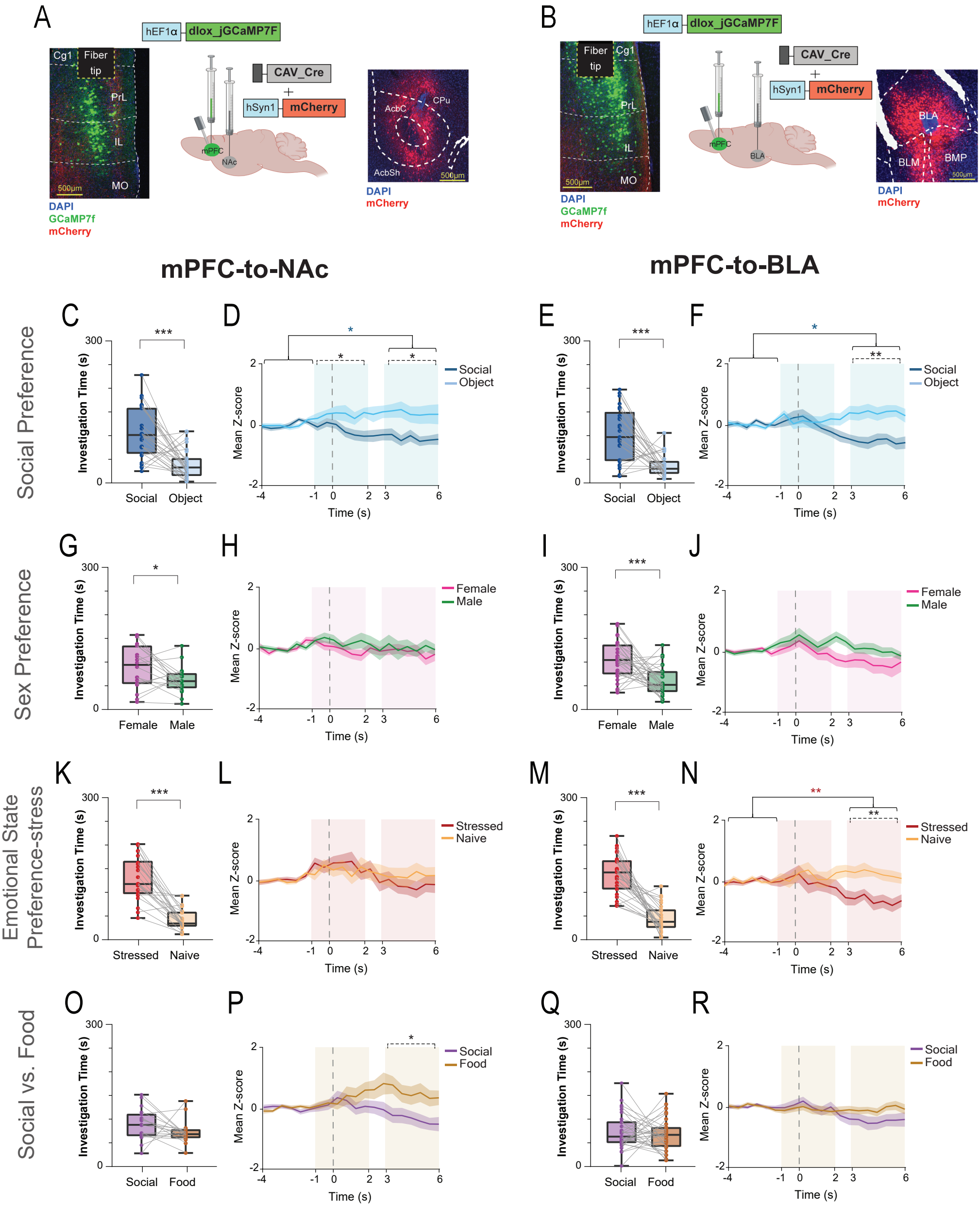
A
hEF1α
dlox_jGCaMP7F
Cg1
Fiber tip
PrL
IL
MO
500μm
DAPI
GCaMP7f
mCherry
CAV_Cre
+
hSyn1
mCherry
mPFC
NAc
AcbC
CPu
AcbSh
B
BLA
BLM
BMP
mPFC-to-NAc
mPFC-to-BLA
Social Preference
Sex Preference
Emotional State Preference-stress
Social vs. Food
C
D
E
F
G
H
I
J
K
L
M
N
O
P
Q
R
Investigation Time (s)
Mean Z-score
Time (s)
Social
Object
Female
Male
Stressed
Naive
Food